International Journal of WILDLAND FIRE
CSIRO PUBLISHING
RESEARCH PAPER
https://doi.org/10.1071/WF25278
International Association of Wildland Fire

Wildfire danger assessment and forecast through fire spread simulations

Jia Yang[A,*], Tyson E. Ochsner[B], Erik S. Krueger[B], Shanmin Fang[A], Quan Zhang[A], Xiaohao Jiao[A], Chris Zou[A], Yongqiang Liu[C], Todd Lindley[D] and Drew Daily[E]

For full list of author affiliations and declarations see end of paper

***Correspondence to:**
Jia Yang
Department of Natural Resource Ecology and Management, Oklahoma State University, Stillwater, OK, USA
Email: jia.yang11@okstate.edu

Received: 21 November 2025
Accepted: 13 June 2026
Published: 28 July 2026

Cite this: Yang J *et al.* (2026) Wildfir e danger assessment and forecast through fire spread simulations. *International Journal of Wildland Fire* **35**, WF25278. doi:10.1071/WF25278

ABSTRACT

Background. Traditional empirical fire danger rating systems are largely based on generalized historical weather-fire relationships. By contrast, fire behavior models incorporate interactions among weather, fuels and topography to simulate fire spread across landscapes, offering opportunities for wildfire danger evaluation. **Aims.** This study is to develop a novel Wildfire Danger Assessment and Forecast (WDAF) framework that estimates daily fire spread potential using spatially explicit fire simulations. **Methods.** The framework integrates weather, fuel and topographic data into a fire behavior model to simulate daily fire sizes. To determine fire danger level for a specific day, the framework compares the simulated fire size for that day against a statistical distribution of fire sizes generated from a multi-year reference period. The simulated daily fire size and its corresponding historical percentile serve as the quantitative metrics to assess fire potential. **Key Results.** Fire potential metrics showed excellent performance in predicting occurrences of large wildfires. WDAF offers several advantages: intuitive fire spread potential quantification, normalization against historical baselines and improved physical realism. **Conclusions.** The framework has strong potential as a complementary tool to existing fire danger rating systems. **Implications.** This study highlights the potential of simulation-based approaches for wildfire danger assessment and forecasting.

Keywords: fire behavior model, fire danger rating system, fire forecast, fire management, fire spread potential, fire regimes.

Introduction

Wildfires play a critical role in shaping vegetation distribution and influencing key biogeochemical and biophysical processes across much of the global terrestrial ecosystems (Krawchuk *et al.* 2009; Yang *et al.* 2015; Coop *et al.* 2016; Yang *et al.* 2017). Although global burned area has exhibited a declining trend over the past two decades (Chen *et al.* 2023), wildfires in the US continues to increase in frequency and intensity (Cunningham *et al.* 2024; MacCarthy *et al.* 2024). These increases are posing escalating threats to human safety, infrastructure and natural resources. In the US, the area of burned forests in the western region increased by 1574 km^2 per decade between 1984 and 2020 (Juang *et al.* 2022), and 84% of ecoregions in the east experienced increases in burned area over the same period (Donovan *et al.* 2023). This pattern is largely driven by a complex interplay of environmental and human factors, such as increased frequency and intensity of fire-promoting weather, changes in fuel structure and loads, and the ongoing expansion of the wildland–urban interface (WUI) (Van Auken 2009; Pausas and Keeley 2021; Chen *et al.* 2024). To enhance the preparedness and effectiveness of fire mitigation strategies, it is critical to have accurate systems to assess both the temporal dynamics and spatial patterns of wildfire potential and to improve the accuracy of holistic fire danger forecasts.

The definition and interpretation of fire danger has evolved considerably over the past 70 years (Hollis *et al.* 2024). In general, fire danger refers to the potential for a fire ignition, spread, fire suppression difficulty, and impact within a specific location and time frame (Sharples *et al.* 2009). Quantifying fire danger involves a series of environmental factors, including fuel type and availability, current and antecedent weather conditions, topography and the presence of ignition sources. Various fire danger indices have been developed to support the planning of prescribed burning, the development of fire management and suppression strategies, and public warning systems. Among the most widely used are the Canadian Fire Weather Index (FWI) system (Van Wagner 1987), the McArthur Forest Fire Danger Index (FFDI) (McArthur 1967), and the Burning Index (BI) from the US National Fire Danger Rating System (NFDRS) (Deeming *et al.* 1977). Over the past 20 years, satellite remote sensing data, such as fuel conditions, topography and meteorological variables, have been increasingly integrated into fire danger rating systems (Pettinari and Chuvieco 2020).

Current empirical derived fire danger rating systems primarily rely on simplified assumptions and generalized relationships between fire and weather conditions (Yeo *et al.* 2015) and do not directly simulate fire outcomes, such as fire size or burned area. For instance, FWI, FFDI and BI are primarily designed to indicate ease of ignition and potential fire spread, but they lack direct simulation of the temporal dynamics of fire behavior and fire spread. Using these indices for risk assessment often relies on predefined thresholds, determined by the percentiles or correlation with historical fire records, to categorize daily fire danger levels (Júnior *et al.* 2022). This approach may experience challenges in regions experiencing novel climate conditions and fuel transitions. Consequently, there is a need for new fire potential assessment tools that can complement or enhance existing fire danger rating systems under shifting climate and fuel conditions (Jolly *et al.* 2024).

Over the past three decades, a variety of fire behavior models have been developed to simulate the spatial and temporal dynamics of wildfire across landscapes, incorporating the influences of topography, fuel conditions, weather and suppression efforts (Ager *et al.* 2011). These models integrate mathematical equations of combustion, heat release and fire spread with dynamic fuel moisture calculations, simulating how fuel moisture changes and a fire front propagates under time-varying weather conditions. One widely used model is the Fire Area Simulator (FARSITE) (Finney 1998), which combines the Rothermel Surface Fire Behavior Model with multiple canopy fire models and incorporates weather, fuel and topographic inputs to produce two-dimensional simulations of wildfire growth and behavior across heterogeneous landscapes. Other well-established fire models that simulate fire behaviors and spread include, but are not limited to, the SPITFIRE model (Thonicke *et al.* 2010), FIRETEC (Koo *et al.* 2012) and Prometheus (Tymstra *et al.* 2010). Advanced coupled models like WRF-Fire (Coen *et al.* 2013) and FIRETEC (Koo *et al.* 2012) capture complex 3D fluid dynamics and fire-atmosphere interactions, providing high physical realism. However, their immense computational demand typically limits their application for the large-scale, near-real-time fire risk forecasting. Process-based models like SPITFIRE (Thonicke *et al.* 2010) are designed to simulate interactions among climate, vegetation and fire at coarse regional to global scales rather than for high-resolution local-scale assessment. In contrast, deterministic spread models such as Prometheus (Tymstra *et al.* 2010) and Wildfire Analyst (Monedero *et al.* 2019) are optimized for rapid execution and operational decision-making. By incorporating spatially explicit data on weather, fuels and terrain, fire models can generate synthetic fire perimeters or fire size under given environmental conditions over a certain period.

Fire behavior models have been widely applied to assess wildfire susceptibility and risk at the landscape level. For example, Bar Massada *et al.* (2009) used the FARSITE model to simulate fire spread in a WUI under both extreme and normal fire weather conditions and estimated burned probability to characterize wildfire risk. Similarly, the BURN-P3 model, developed from the Canadian Fire Behavior Prediction System, has been used to simulate long-term burn probability and baseline wildfire susceptibility (Parisien *et al.* 2005). While recent efforts have begun to use fire spread simulations for near real-time prediction (Oliveira *et al.* 2023), simulation-based metrics from fire behavior models remain underutilized for operational daily fire danger assessment and forecasting. This gap is partly due to computational demands, the need for high-resolution spatiotemporal data and the lack of standardized methodologies to translate simulated model outputs into fire potential metrics. Recent advances in weather forecasting and reanalysis products, satellite-derived fuel characterization (Rollins 2009), and fire behavior models (Finney 1998) opens new opportunities to address these barriers and support the operational use of simulation-based daily fire danger quantification.

This study aims to: (1) develop a novel framework for daily fire spread potential assessment and forecast that leverages spatially explicit fire size simulations generated by a fire behavior model; and (2) demonstrate its implementation through a case study in the Southern Great Plains (SGP), US, and evaluate the framework's forecasting skill in predicting fire spread potential using weather forecasts. Additionally, we examine both the challenges and potential in the operational application of this framework for fire danger forecast. Because focus of this study is on evaluating the potential of fire behavior models to quantify fire spread as a proxy of fire danger level, we emphasize model outputs of daily fire size rather than other variables, such as fireline intensity or flame length.

Materials and methods

Structure of the Wildfire Danger Assessment and Forecast (WDAF) framework

The Wildfire Danger Assessment and Forecast (WDAF) framework developed in this study relies on simulations of fire spread and daily fire size using a fire behavior model (Fig. 1). Daily fire size in this study is defined as the area burned by a hypothetical fire that ignites at midnight and spreads over a 24 h period. For a given area, users select a multi-year reference period to run daily simulations of multiple hypothetical wildfires and generate statistical distributions of daily fire size. To assess fire danger (i.e. fire spread potential in this study) on a specific day, simulations are conducted using the fire model and input weather conditions for that day, and the resulting fire sizes are compared against the reference distributions to determine the fire danger level. Our approach is based on the premise that fire size is among the most robust indicators for fire impact and danger level, providing a tangible metric that directly reflects fire risk under given environmental conditions (Walding *et al.* 2018; Tedim *et al.* 2018; Balch *et al.* 2024). Specifically, the evaluation and forecasting of fire spread potential for a given area consists of six steps (Fig. 1):

- Step 1: prepare input data for the fire behavior model, including hourly weather data (temperature, precipitation, relative humidity, wind speed, wind direction and cloud cover) for the multi-year reference period, topography (elevation, slope, aspect), surface and canopy fuel characteristics (fuel type, fuel loading for live fuel and dead fuel, fuel bed depth, canopy height, base height, canopy density, coverage) and hypothetical ignition points.
- Step 2: run fire behavior simulations to estimate the spread and daily size of the hypothetical fires throughout the reference period, spanning multiple years.
- Step 3: generate statistical distributions of simulated daily fire size from the reference simulations.
- Step 4: prepare hourly weather data for the target day of interest.
- Step 5: run the fire behavior model using the target day's weather data to simulate the daily size of hypothetical fires.
- Step 6: assess fire danger by comparing the simulated fire size for the target day against all simulated daily fire sizes during the reference period and calculating the corresponding percentile values.

This WDAF framework is flexible, which requires users to configure parameters based on regional environment conditions and available computational resources. Users need to select a fire behavior model commensurate with available computational resources and spatial data resolution, define a multi-year reference period sufficient to capture fire danger interannual variability, set a simulation grid size that balances spatial heterogeneity with processing time constraints, evaluate statistical functions using goodness-of-fit metrics to model local fire size distributions and define percentile thresholds to quantitatively categorize fire danger levels.

Demonstration of the WDAF framework

The Southern Great Plains (SGP) – area for demonstration

We selected the three states of Kansas, Oklahoma and Texas in the SGP (Fig. 2), which are characterized by the fastest fire spread in the US (Balch *et al.* 2024; Fang *et al.* 2026), to demonstrate the application of the WDAF framework to quantify fire danger levels both retrospectively and in a short-term forecast mode. According to the fuel type map based on the Scott and Burgan 40 fuel models developed by the LANDFIRE project (Rollins 2009), six major fuel types are present across the land area of the three states: NB (Nonburnable, 25.2%), GR (Grass, 44.7%), GS (Grass-Shrub, 16.2%), SH (Shrub, 1.5%), TU (Timber-Understory, 1.9%) and TL (Timber Litter, 10.5%) (Fig. 2). Note that the NB category primarily includes urban areas, agriculture fields and bare ground. The NB category is more prevalent in Kansas, the central and western regions of Oklahoma, and the Texas Panhandle, as well as in some metropolitan areas in Texas, including Dallas, Austin and Houston (Supplementary Fig. S1). It is noteworthy that during the crop growing season, agriculture fields classified as NB can act as barrier to fire spread; however, outside of the period, they may contribute to fire spread. The GR category is widely distributed across the entire domain, while the GS is concentrated in western and southwestern Texas. In contrast, the TL category is more prevalent in the eastern portion of the three states.

The land area of the three states was divided into 429 hexagons, each with a side length of 31 km and an area of 2500 km^2. These hexagons were used as the basic units in this demonstration for simulating fire spread and daily fire size, evaluating wildfire danger and forecasting fire risk. Hexagons with more than 50% of NB land were excluded, resulting in a final set of 356 selected hexagons to show the spatial pattern of fire danger levels across the three states. This exclusion was a methodological necessity driven by the static nature of the LANDFIRE dataset, which maps agricultural fields as NB year-round. Because FARSITE cannot simulate fire spread across NB pixels, heavily agricultural hexagons often yielded zero or very small daily fire sizes, preventing the development of a reliable fire danger evaluation for those specific cells. Fire spread and daily fire size simulations were conducted for each hexagon. Under extreme fire weather conditions, fires could spread beyond

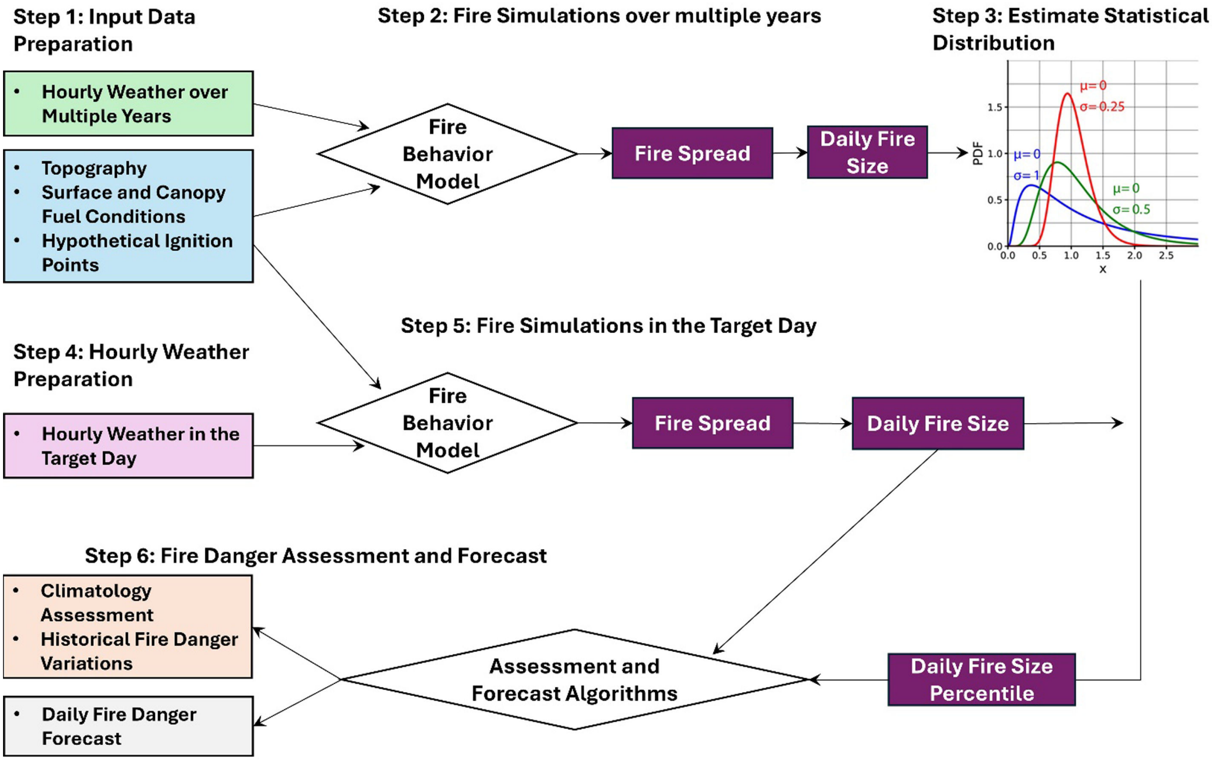

Fig. 1. Diagram of the Wildfire Danger Assessment and Forecast (WDAF) framework based on simulations of fire spread and daily fire size. The fire behavior model in the framework acts as the core engine to simulate two-dimensional spatial fire growth and fire size.

hexagon boundaries. To account for this, we applied a 10 km buffer outside each hexagon to mitigate the edge effects.

Additionally, four hexagons (Fig. 3) were selected to present a time series of fire danger levels and to evaluate the effectiveness of the developed WDAF framework in capturing the occurrence of four large wildfires. These hexagons included the Smokehouse Creek Fire (26 February 2024) in Roberts County, Texas; the Rhea Fire (13 April 2018) in Dewey County, Oklahoma; the Starbuck Fire (6 March 2017) in Beaver County, Oklahoma; and the Cottonwood Fire (14 March 2025) in Payne County, Oklahoma. The Rhea Fire and the Starbuck Fire were used to assess the WDAF framework's capacity to detect elevated fire danger levels on the days when extreme fire events occurred. In contrast, the Smoke Creek Fire and the Cottonwood Fire were used to evaluate the WDAF framework's potential, in combination with weather forecasts, to predict elevated fire danger levels several days in advance. The Smokehouse Creek Fire, the Rhea Fire and the Starbuck Fire are three major megafires in the SGP, resulting in tremendous economic losses and structure damage. The Smokehouse Creek Fire, the largest wildfire in Texas history, burned approximately 1,058,482 acres (4283 km^2) in the Texas panhandle and western Oklahoma. The Rhea Fire, one of the largest wildfires in Oklahoma history, burned approximately 286,196 acres (1148 km^2) and caused significant damage to homes and infrastructures in western Oklahoma. The Starbuck Fire scorched approximately 660,000 acres (2671 km^2) across parts of Kansas and Oklahoma.

Fire behavior model and input data preparation

In principle, any fire behavior model capable of simulating fire spread and fire size can be integrated into the WDAF framework. For demonstration purposes, we employed the FARSITE model (Finney 1998), which simulates fire growth based on hourly weather data. FARSITE accounts for both surface and canopy fire behavior and dynamically models hourly fuel moisture. Required inputs include fuel type distribution, topography, hourly weather conditions and ignition locations.

The 30 m fuel type map from the LANDFIRE project (LF2022_FBFM40_230; Fig. 2) was used to drive FARSITE in this demonstration, which was developed based on the 40 Scott and Burgan Fire Behavior Fuel Models (Scott and Burgan 2005). The procedures for deriving surface fuel and canopy fuel characteristics are detailed in Rollins (2009). Topographic input at 30 m resolution, including elevation, slope and aspect, was also obtained from the LANDFIRE project, which was developed based on the USGS 3D Elevation Program (3DEP). We observed that the 30 m LF2022_FBFM40_230 fuel type data captured the

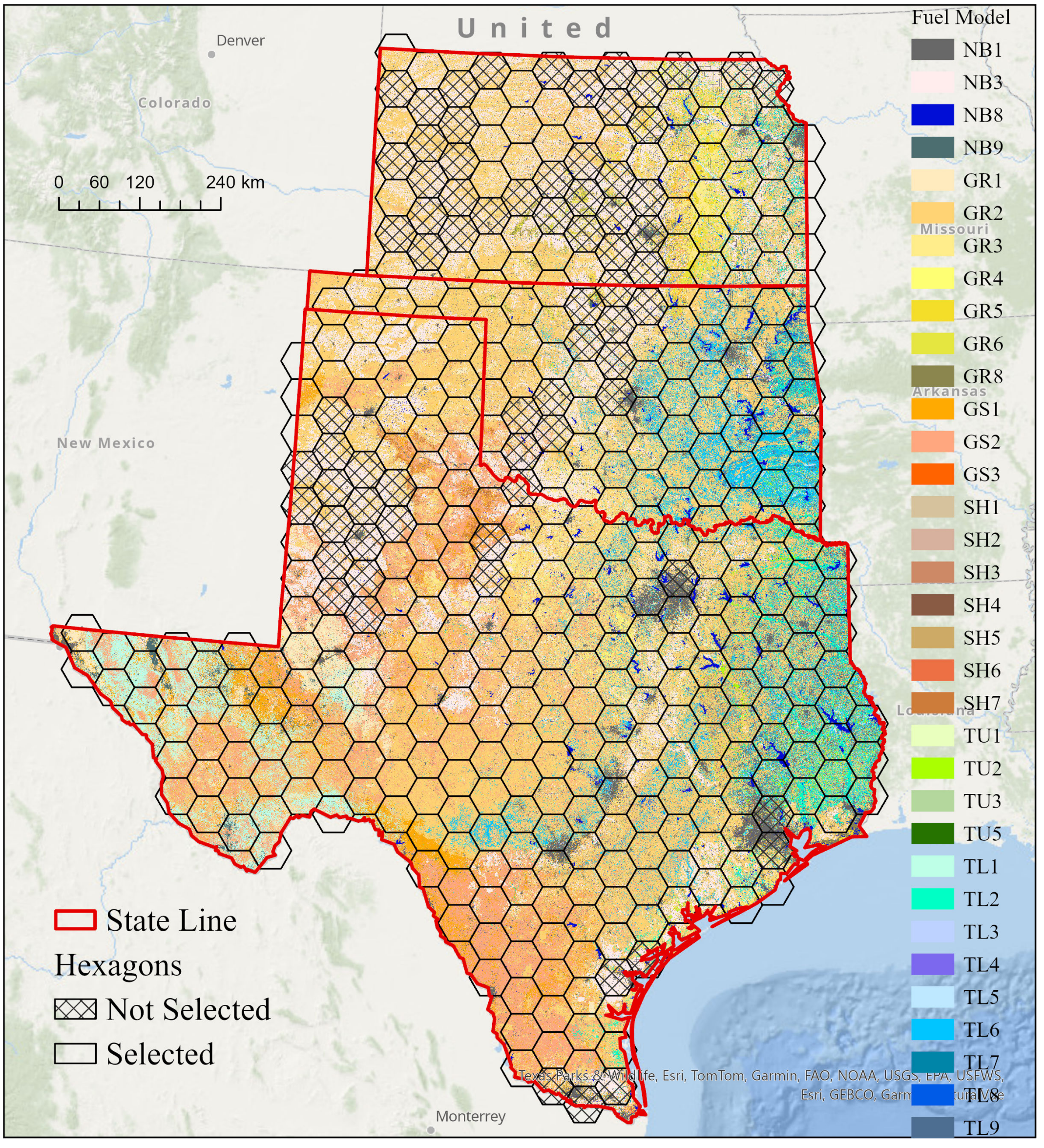

Fig. 2. Study area covering the Southern Great Plains region of the US, including the states of Kansas, Oklahoma and Texas (north to south). Hexagons with hatching indicate areas excluded from wildfire danger assessment and forecast due to a high proportion of nonburnable land (such as urban, agriculture field and bare ground). Fuel types are based on the 40 Scott and Burgan Fire Behavior Fuel Models from the LANDFIRE project. For detailed descriptions of the fuel models, see Scott and Burgan (2005). Numbers in the legend indicate variations within the same fuel type, denoting differences in fuel parameters such as fuel loading and fuelbed depth. NB, Nonburnable; GR, Grass; GS, Grass-Shrub; SH, Shrub; TU, Timber-Understory; TL, Timber Litter.

distribution of roads, which act as potential barriers to fire spread by reducing the likelihood of fire spreading across them. However, in many wildland areas, minor roads are typically narrow and may not function as effective fuel breaks (Bar Massada *et al.* 2009). To address this, we obtained secondary road data from the US Census Bureau's TIGER/Line database and replaced NB pixels intersecting these secondary roads with the nearest adjacent fuel type. This adjustment allows for more realistic fire spread simulations in the wildland areas. This approach is similar to that of Bar Massada *et al.* (2009), who replaced smaller roads with short grass to better represent the burnable conditions.

Hourly weather conditions were obtained from two sources: the North American Regional Reanalysis (NARR; Mesinger *et al.* 2006) and the North America Mesoscale (NAM) Forecast System. NARR data was used to drive FARSITE during the 7 year reference period (2016–2022) to

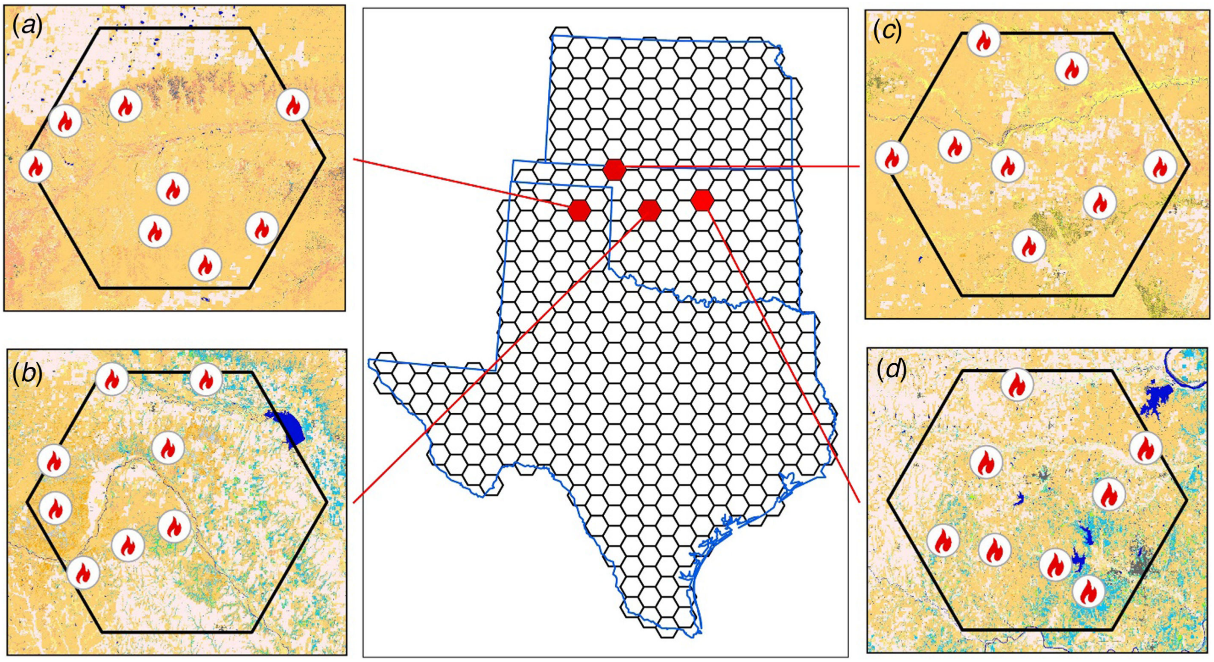

Fig. 3. Selected hexagons used to demonstrate the capacity of the new framework to quantify fire danger levels for four wildfire events: the Smokehouse Creek Fire in Roberts County, Texas (*a*); the Rhea Fire in Dewey County, Oklahoma (*b*); the Starbuck Fire in Beaver County, Oklahoma (*c*); and the Cottonwood Fire in Payne County, Oklahoma (*d*). Each hexagon contains eight randomly distributed hypothetical ignition points for simulating fire spread and daily fire size. The fuel model legend is the same as in Fig. 2.

generate statistical distributions of simulated fire size for each selected hexagon. This period encompasses both dry and wet years, as well as years with extensive burned area and years with only small to medium burned area. It was considered sufficient to capture variability in weather and interannual climate conditions and was used as a reference period to represent fire danger climatology. In this study, fire danger climatology refers to the multi-year average conditions of fire danger levels and the associated range of variability, which include maximum, median and interquartile range (IQR) of the simulated daily fire sizes. In contrast, NAM weather forecast data were used to drive FARSITE simulations for the target day to support fire danger forecasting. Weather variables used to drive the WDAF system include hourly temperature, precipitation, relative humidity, wind speed, wind direction and cloud cover.

Additionally, eight randomly distributed ignition points were placed within each selected hexagon to simulate fire spread (Fig. 3). This number was chosen to capture the spatial variations of topography and fuel conditions within each hexagon while keeping computational demands manageable. If an ignition point fell on an NB land cover type or was surrounded by NB pixels, fire spread could not occur. In such cases, the ignition point was removed and replaced with a new one to ensure valid fire simulations. Given the considerable variability in fuel types and topography within a single hexagon, using multiple ignition points and calculating the average characteristics of these fires are essential to adequately capture this spatial heterogeneity and its influence on fire spread. Additionally, a minimum distance of 5 km was enforced to prevent ignition points from being placed too close to one another. We ran simulation separately for each fire to avoid the conflation of distinct fire events. Finally, the average size of the eight hypothetical fires was calculated to represent the generalized daily fire size in the hexagon.

We acknowledge that in reality, ignition sources are not randomly distributed; they occur more frequently in the WUI and near roads. However, a strategy that concentrates ignitions in WUI areas can substantially limit fire spread, potentially leading to an underestimation of fire size and spread potential in wildland areas. To avoid this artificial truncation, we adopt a strategy of randomly placing ignition points across burnable pixels in the hexagon to provide a generalized assessment of spread potential across the entire landscape.

Fire model simulation procedure

In Step 2 and Step 5 of the WDAF framework (Fig. 1), we ran the FARSITE model for each ignition point over a 48 h period, covering both the current day for fire danger evaluation and the preceding day. Because the moisture content of dead fine fuels (1 and 10 h fuels) strongly influences fire behavior and fire spread (Rodrigues *et al.* 2024) and is highly sensitive to antecedent weather conditions, we included a 24 h FARSITE simulation using weather data from the preceding day to better simulate fuel moisture dynamics in the current day. Initial dead fuel moisture contents at midnight (local time) on the preceding day were set to 6, 7, 8 and 16% for the 1, 10, 100 and 1000 h fuels, respectively, and were subsequently updated by FARSITE based on hourly weather inputs. Live fuel moisture content was set at 80% for herbaceous fuels and 90% for woody fuels. These initial dead and live fuel moisture values are based on FARSITE's default setting, which may introduce uncertainty into the simulated fire size. When available, users should incorporate observed fuel moisture data from field measurements, remote sensing, or continuous fuel moisture simulations to improve simulation accuracy. Fires were assumed to start at midnight (local time) on the current day and burn continuously for 24 h. For the fire danger forecasting, we used NAM weather data issued 24 h in advance of the target evaluation day. For example, the NAM weather forecast issued at midnight (local time) on 13 March was used to run the WDAF for the subsequent 48 h and forecast fire danger levels for 14 March, when the Cottonwood Fire occurred.

Statistical distribution functions

Step 3 of the WDAF framework involves selecting an appropriate statistical distribution function and fitting its parameters for each hexagon to characterize the distribution of simulated daily fire size during the reference period. Fire sizes typically exhibit right-skewed distributions, with many small fires and fewer large fires. Commonly used statistical models to represent such distributions in fire science include the log-normal distribution (Yang *et al.* 2015; Hantson *et al.* 2016) and exponential distribution (Cumming 2001).

We evaluated both log-normal and exponential distribution functions across multiple hexagons in the SGP states. A representative result is shown in Fig. 4, which depicts the distribution of daily fire sizes from 2016–2022 within a hexagon located in Roberts County, Texas (Fig. 3*a*). Both distributions performed well in fitting the histogram, as shown by the Kolmogorov–Smirnov (KS) test statistics: 0.0868 for the log-normal fit and 0.0646 for the exponential fit (both with P-values = 0.00). The KS test measures the maximum difference between the data distribution and the theoretical distribution function; lower KS statistics indicate a closer fit. These results suggest that either function can reasonably represent the distribution of fire sizes. However, the log-normal function exhibits a higher probability density when the daily fire size is near zero, which more closely resembles the histogram. Therefore, we selected the log-normal distribution in the SGP to fit the distribution and to estimate the percentile of fire size. The log-normal probability distribution function (PDF) for daily fire sizes is:

$$f(x) = \frac{1}{(x - loc)\cdot\sigma\cdot\sqrt{2\pi}}\exp\left[-\frac{\left(\ln(x - loc) - \mu\right)^2}{2\sigma^2}\right].$$

where x is the simulated daily fire size plus 0.01 (in km^2) to ensure all values are positive, and σ, loc and μ are the three parameters that define the shape, location and scale of the distribution. These parameters vary across hexagons. For the hexagon in Fig. 3*a* during the reference period, σ = 1.3601 , loc = –0.1235– and μ = 1.201.

Wildfire danger assessment and forecast

Variations in daily fire size are an important indicator of fire danger level, as fire size generally increases monotonically with the fire danger index (Walding *et al.* 2018). In this study, simulated daily fire size is used as one metric to quantify fire danger. However, fire size exhibits substantial spatial variability due to regional differences in climate conditions, topography and vegetation types (Andela *et al.* 2019). To better capture the temporal dynamics of fire danger within a specific region, we calculate the relative daily fire size – expressed as the percentile of the target day's fire size based on the fitted probability distribution function (section Statistical distribution functions). This percentile value serves as an additional metric for quantifying fire danger.

NFDRS Burning Index

BI is one of the most widely used indicators for quantifying fire danger and difficulty of fire suppression in the US and is employed by systems such as Wildland Fire Assessment System, OK-FIRE (Carlson *et al.* 2002) and Texas A&M Forest Service. The estimation is based on the integration of both the Spread Component (SC) and the Energy Release Component (ERC) (Deeming *et al.* 1977; Jolly *et al.* 2024). As spread potential is a major component in BI, we selected BI in this study to compare with daily fire size simulations in the WDAF. In this study, we obtained daily BI values from the 4 km resolution gridMET (Abatzoglou 2013), which were developed using Fuel Model G in NFDRS 77 (Cohen and Deeming 1985). Because the WDAF estimates fire potential at the scale of 2500 km^2 hexagons, we performed a spatial aggregation by calculating the mean BI value across all 4 km grid cells that intersected each respective hexagon. These upscaled BI values were then compared with the fire metrics generated by the WDAF framework. It is acknowledged that the simulated fire size is a physical, dimensional metric (km^2) while BI is a unitless index. The comparison between the two metrics is not intended to establish a direct numerical equivalence. Rather, the objective is to quantify whether the temporal variations and sensitivity to fire-conducive environmental conditions captured by the

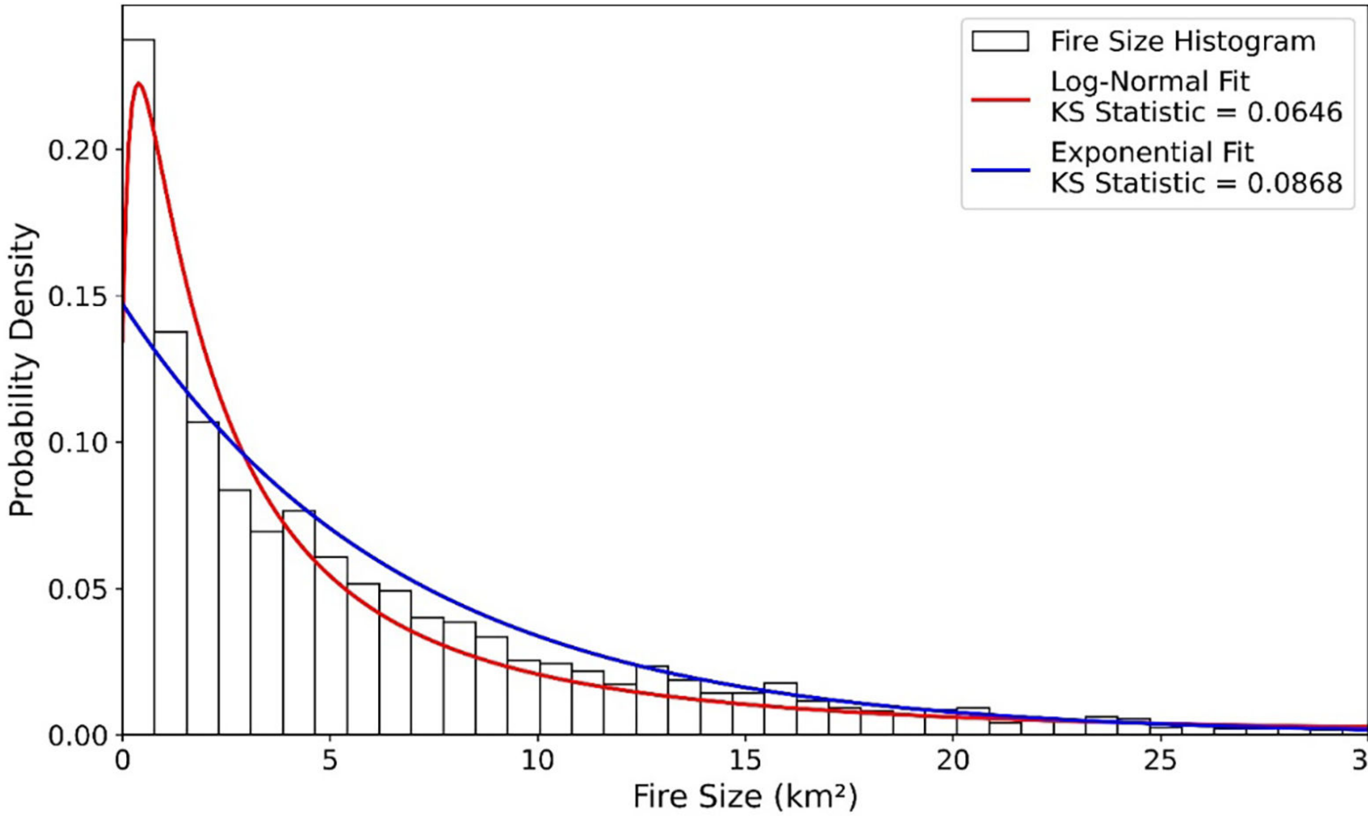

Fig. 4. Histogram of simulated daily fire sizes for the hexagon in Roberts County, Texas during 2016–2022, along with fitted distribution curves based on the log-normal and exponential functions. The goodness-of-fit was evaluated using the Kolmogorov–Smirnov (KS) test statistics.

physically-based WDAF framework align with the well-established, operational fire danger patterns represented by BI.

To facilitate the comparison, we randomly selected nine hexagons (H1–H9) across the study area (Supplementary Fig. S2), representing a wide range of locations, climate conditions, topography and vegetation types. The time series of simulated daily fire size, fire size percentile and BI for the nine selected hexagons are presented in Supplementary Figs S3–S5, respectively. For each hexagon, we applied Spearman's rank correlation to evaluate whether the simulated fire size and BI co-varied over time. Additionally, we applied shape-constrained additive models (SCAM) to investigate the nonlinear, monotonic relationships between BI and two WDAF-derived fire danger metrics: daily fire size and fire size percentile, across nine representative hexagons. SCAMs were selected for their flexibility in modeling complex, nonlinear patterns without requiring a predefined functional form (Pya and Wood 2015). We implemented the models with the 'mgcv' and 'scam' packages in *R*, specifying a Gamma family and log link function to model the right-skewed distribution of BI (Wood 2017). Separate SCAMs were fitted for each hexagon to examine the relationship between BI values and fire size (or fire size percentile). To assess model performance, we calculated the adjusted R^2 for each fitted SCAM to provide a quantitative measure of explanatory power.

Monitoring Trends in Burn Severity (MTBS) dataset

The Monitoring Trends in Burn Severity (MTBS) project provides a long-term dataset, dating back to 1984, that maps the location, perimeter and severity of large wildfires in the US. (Eidenshink *et al.* 2007). It includes fires with sizes over 500 acres in the eastern US and 1000 acres in the western US. Using Landsat satellite imagery, MTBS quantifies pre- and post-fire vegetation conditions to derive burn severity and delineate burned areas. This dataset has been widely used to offer valuable information on fire extent and severity over time (Picotte *et al.* 2016; Ivey *et al.* 2024). In this study, we extracted MTBS wildfire occurrence data for Kansas, Oklahoma and Texas from 2016–2022, encompassing a total of 414 large fire events (Supplementary Fig. S6). These wildfire records were used to as 'ground truth' data to evaluate the effectiveness of fire potential metrics in predicting the occurrences of large wildfires. Additionally, this data was also used to compare the wildfire spatial patterns with the climatology of fire danger levels generated by the WDAF framework during the period of 2016–2022.

Statistical methods to evaluate the effectiveness of fire danger metrics

Fire danger metrics should effectively capture variations in fire-prone environmental conditions. In this study, we employed two statistical methods to evaluate the predictive performance of BI, daily fire size and fire size percentile in predicting the occurrences of large wildfires. The two methods are (1) the Receiver Operating Characteristic (ROC) curve and the associated Area Under the Curve (AUC) (Bradley 1997), and (2) the lift value (Choudhary and Gianey 2017). The ROC curve shows the relationship between True Positive Rate versus False Positive Rate, while the AUC quantifies the overall capacity of each metric to discriminate fire and non-fire events. An AUC value of 0.5 indicates no predictive skill, whereas a value of 1.0 represents perfect discrimination. The lift value quantifies the improvement of fire danger metrics over random guessing, expressed as the ratio of the wildfire occurrence rate within the top *x*% of each fire potential metric to the overall fire occurrence rate. A higher lift indicates greater effectiveness in identifying the most fire-prone conditions. In this study, lift values were calculated for each metric at 10 percentile levels (top 10, 20, …, 100%).

Based on the spatial coordinates and ignition dates of wildfires from the MTBS dataset (Supplementary Fig. S6), we extracted fire records and their associated BI, the simulated daily fire size and fire size percentile. To provide a comparison, we also randomly selected non-fire records and the retrieved BI, daily fire size and fire size percentile. These fire and non-fire records were then used to compute AUC and lift values.

Results

Fire danger assessment

Correlation between WDAF fire metrics and Burning Index

During the assessment period between 2016 and 2022, we analyzed a total of 2557 days of simulated fire size and fire size percentile data (Supplementary Figs S3 and S4). These fire metrics were compared with BI across nine randomly selected hexagons in the SGP (see their location in Supplementary Fig. S2). Across the nine hexagons, Spearman's correlation coefficients ranged from 0.638 to 0.773 between BI and daily fire size, and from 0.639 to 0.774 between BI and fire size percentile (Table 1). All correlations were statistically significant (P-value < 0.001). The strong and consistent correlations indicate that the WDAF metrics capture the daily variations in fire-conducive weather conditions represented by BI. This high correlation is not intended to suggest that WDAF demonstrates better performance, nor does it treat BI as an absolute 'true' reference. Instead, it shows that the WDAF framework produces reasonable danger assessments consistent with NFDRS operational fire indices. Since fire size percentile is a monotonic function of fire size, it is not surprising that Spearman's correlation coefficients between BI and fire size are similar as that between BI and fire size percentile (Table 1).

The SCAM plots revealed a consistent, positive and nonlinear relationship between BI and the simulated daily fire size across all nine hexagons (Fig. 5). Overall, BI increased with fire size; however, the rate of increase varied across different fire size ranges. BI was more responsive to changes in the simulated fire size when fire size was relatively small (for example, less than 5 km^2/day), showing a steep increase with a small increment in fire size. In contrast, at medium to large fire sizes, the rate of BI increase became more gradual, suggesting a reduced sensitivity of BI to further increases in fire size. Adjusted R^2 values for the SCAMs ranged from approximately 0.34–0.43 across the hexagons, indicating that the model explained a substantial portion of the variability in BI. These results support the potential of WDAF-derived daily fire size as a predictor of fire danger, consistent with the operational fire ratings reflected in BI.

It is noteworthy that significant differences emerge when daily fire sizes are relatively small (Fig. 5), primarily due to a noticeable gap in BI values between 0 and approximately 20. This gap suggests that BI may lack sensitivity to variations in fire danger under low fire potential conditions. In contrast, the simulated fire sizes exhibit no such gap, indicating that they provides a continuous sensitivity to variations in fire danger under low fire potential conditions, offering a complementary perspective to traditional empirical fire danger evaluation system. The frequent occurrence of zero BI values under mild conditions might be an artifact of the spatial scaling and fuel model selection (model 'G') inherent to the gridMET BI data. When environmental conditions result in higher fuel moisture above extinction threshold of model 'G' (i.e. 25%), the calculated BI drops to zero. In contrast, the WDAF framework simulates fire behavior using 30 m high-resolution LANDFIRE data, which captures the significant heterogeneity in fuel moisture due to spatial variations in fuel types and topographic conditions within the same area. Therefore, even under mild weather conditions, FARSITE can still simulate fire spread in areas with fuel moisture below the extinction threshold and generate a non-zero fire size simulation.

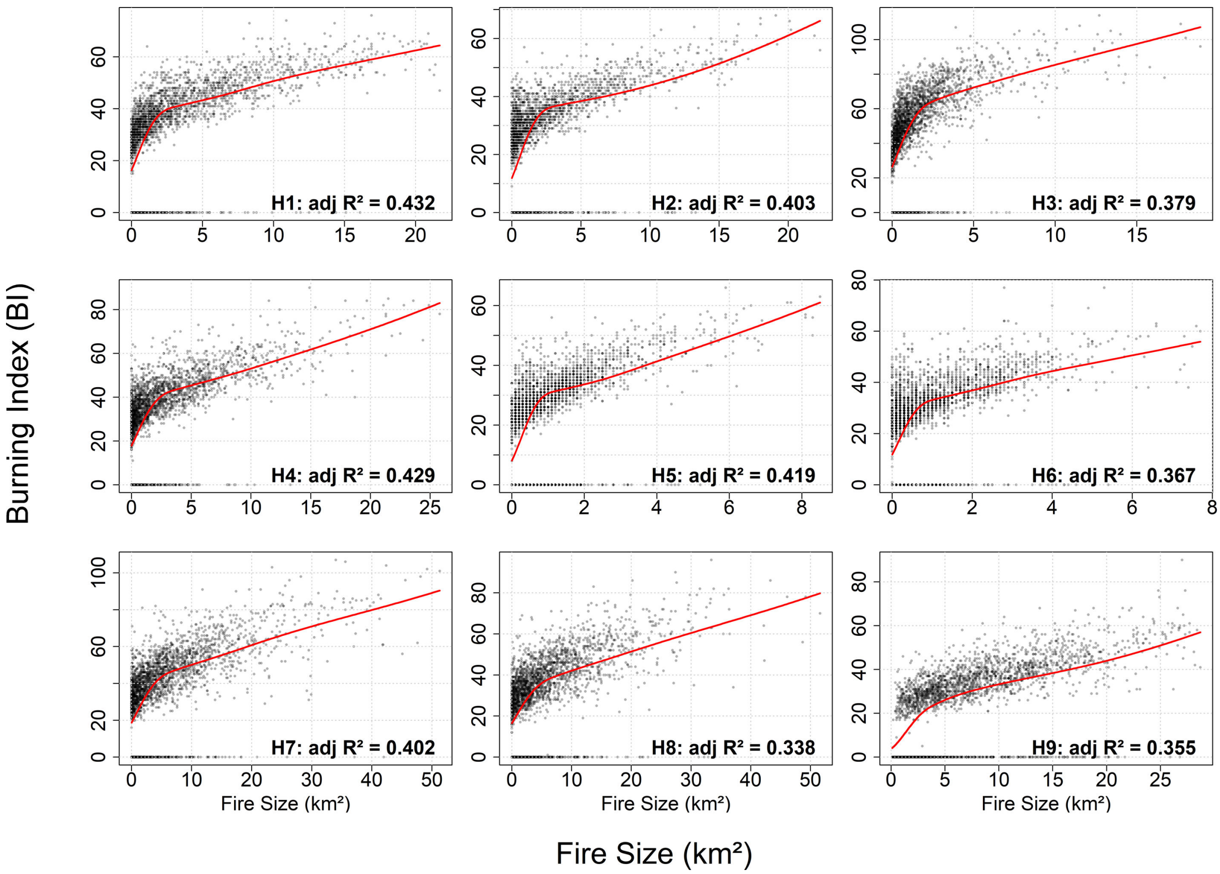

Fig. 5. Shape-constrained additive model (SCAM) fits of the Bburning Index (BI) as a function of simulated daily fire size (km^2) across nine selected hexagons (H1–H9) in the southern great plains (see Supplementary Fig. S2). Each panel shows a scatterplot of BI against fire size (black dots) and a fitted SCAM curve (red line).

Table 1. Spearman's correlation coefficients between Burning Index (BI) and daily fire size and between BI and fire size percentile.

Hexagon	BI : Fire size	BI : Percentile
H1	0.773***	0.774***
H2	0.716***	0.718***
H3	0.713***	0.714***
H4	0.732***	0.735***
H5	0.713***	0.716***
H6	0.673***	0.68***
H7	0.687***	0.687***
H8	0.638***	0.639***
H9	0.658***	0.658***

Note: H1–H9 are the nine selected hexagons (see Supplementary Fig. S2). ***Indicates that coefficients are statistically significant at the level $P < 0.001$.

The SCAM results also revealed a strong and nonlinear positive relationship between BI and fire size percentile across the hexagons (Fig. 6). While BI generally increased with fire size percentile, the rate of increase varied across the percentile spectrum. Compared to the scatterplots of BI versus daily fire size (Fig. 5), the data points in the BI–percentile plots were more evenly distributed across the full range of percentiles, which allows for clearer pattern detection. The fitted SCAM curves commonly exhibited two key inflection points (typically around the 30th–40th and near the 80th percentiles), indicating changes in the sensitivity of BI to changes in fire size percentile. At low percentiles (below ~ 40%), BI rose more sharply with increasing percentile. In the middle range between the 40th and 80th percentiles, the BI increase rate was reduced. Beyond the 80th percentile, BI again increased more rapidly. This reduced rate of BI increase in the middle range suggests that under moderate fire weather conditions, the metric of fire size percentile from WDAF is more sensitive to minor shifts in weather conditions, which interact with localized fuel conditions to produce a large variation in the simulated fire size. This phenomenon underscores the value of the simulation-based approach as a complementary tool to detect fire danger that BI may overlook. Adjusted R^2 values ranged from 0.34 to 0.47 across the hexagons, consistently higher than those from the BI-fire size models, which suggests that the fire size percentile provides a more effective predictor of BI variability than fire size. Overall, these results show that the percentile-based metric from the WDAF framework aligns with the daily fire danger patterns represented by BI, establishing a baseline of validity for the simulation-based approach.

Effectiveness in predicting the occurrences of large wildfires

The predictive capacity of BI, WDAF daily fire size and fire size percentile in capturing the occurrences of large wildfires across the SGP was evaluated using the AUC and lift values (Fig. 7). All three metrics demonstrated powerful skills in discriminating between fire and non-fire conditions, with AUC values of 0.729 for BI, 0.761 for daily fire size and 0.805 for fire size percentile. Among them, the fire size percentile exhibited the strongest overall predictive performance, consistent with its highest AUC and lift values. Specifically, the lift value for the top 10% of predictions reached 1.98 for fire size percentile, compared to 1.87 for daily fire size and 1.79 for BI, indicating a nearly twofold higher likelihood of large wildfire occurrence under the most fire-prone conditions. These results show that the fire size percentile-based and fire size-based metrics derived from the WDAF framework provided good performance in estimating the occurrence of large wildfires, highlighting the complementary value of the spatially explicit WDAF framework by providing managers with an additional, physically intuitive assessment of fire potential.

Assessment of fire danger for the Rhea Fire (2018) and Starbuck Fire (2017)

To evaluate the capacity of the WDAF framework in capturing the occurrences of large fires, we examined two major fire events in the SGP: the 2018 Rhea Fire and the 2017 Starbuck Fire. The critical growth dates for these events were 13 April 2018 for the Rhea Fire and 6 March 2017 for the Starbuck Fire, representing the periods of most rapid fire expansion and highest operational concern (Lindley *et al.* 2019). On 13 April 2018, the simulated daily fire size in the Rhea Fire hexagon (located in Dewey County, Oklahoma) reached 19.4 km^2, placing it at the 95.6th percentile of all simulated daily fire size values from 2016–2022 (Figs 8 and 9). Likewise, on 6 March 2017, the simulated daily fire size in the Starbuck Fire hexagon (in Beaver County, Oklahoma) reached 35.4 km^2, corresponding to the 96.1st percentile. These substantial daily fire sizes and their high percentiles underscore the WDAF's effectiveness in detecting the timing and magnitude of extreme fire behavior during large fire events.

Assessment of fire danger climatology

To further evaluate the effectiveness of WDAF-derived fire metrics in capturing fire danger levels, we analyzed the climatology of fire danger across the study area using simulated daily fire size from 2016–2022. This analysis includes key statistical summaries, including maximum, median and IQR of daily fire sizes, providing a spatial overview of fire danger characteristics across the region (Fig. 10). Results indicate that the highest maximum daily fire sizes are primarily distributed in the Oklahoma and Texas Panhandle regions and the Flint Hills of eastern Kansas, with many hexagons exceeding 70 km^2/day (Fig. 10*a*). A west-to-east gradient is apparent, with generally larger maximum fire sizes in the west and smaller sizes in the east. This pattern reflects underlying differences in the abundance of herbaceous fuel, land cover types and climatic dryness. The IQR of daily fire sizes is an indicator of the temporal variability in the simulated fire sizes and associated fire danger levels. Similar to the spatial pattern of maximum fire sizes, the IQR reaches its highest values in the Flint Hills and the Oklahoma and Texas Panhandle regions (Fig. 10*c*), highlighting areas with greater day-to-day, seasonal and interannual variability in fire danger levels.

The median daily fire sizes show a different spatial pattern compared to the maximum daily fire sizes. The median fire sizes are generally higher in the western portion of the region, particularly in western Oklahoma and Texas Panhandle area. The highest median fire sizes are observed in the Flint Hills of eastern Kansas, typically exceeding 7 km^2/day (Fig. 10*b*). This indicates that fire danger levels in the Flint Hills, western Oklahoma, and the Texas Panhandle are consistently high, aligning with the spatial pattern of MTBS wildfire occurrences (Supplementary Fig. S6), which also shows a high frequency of large fires in these areas. The elevated fire activity is likely driven by a combination of abundant herbaceous fuel and frequent severe fire weather, making these regions among the most fire-prone regions (Baker *et al.* 2019). Hexagons in the eastern part of the SGP exhibit low median fire sizes, indicating a generally lower fire danger level in this region. This pattern is likely influenced by the relatively wetter climate and a higher proportion of forested land cover, both of which will enhance fuel moisture and reduce fire susceptibility.

Fire danger forecast for the Smokehouse Creek Fire (2024) and Cottonwood Fire (2025)

Driven by NAM weather forecasts, we used the WDAF to simulate daily fire sizes across the SGP for two days of 26 February 2024, and 14 March 2025 (Fig. 11), which correspond to the critical growth dates of the Smokehouse Creek Fire and the Cottonwood Fire, respectively. The Smokehouse Creek Fire, which started in the Texas Panhandle

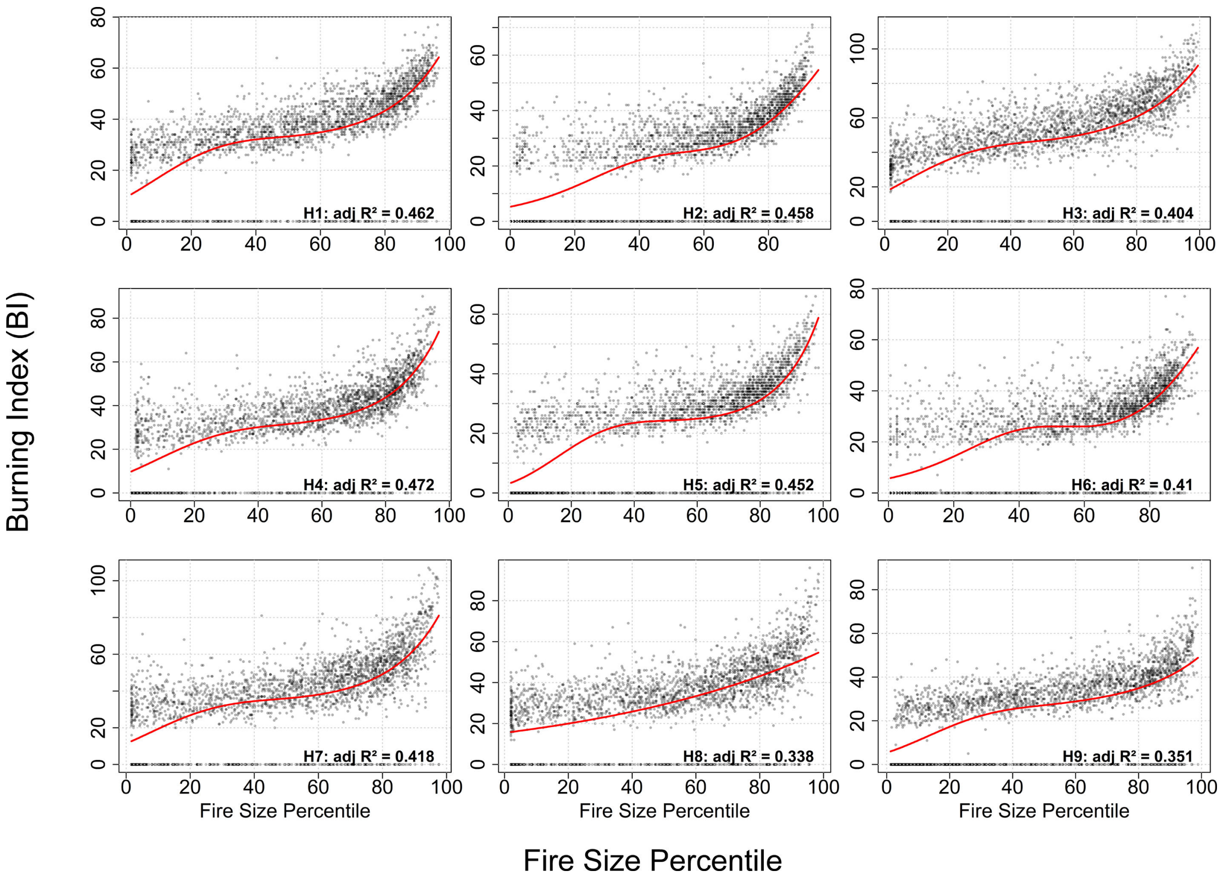

Fig. 6. Shape-constrained additive model (SCAM) fits of the Burning Index (BI) as a function of simulated daily fire size percentile across nine selected hexagons (H1–H9) in the Southern Great Plains (SGP) (see Supplementary Fig. S2). Each panel shows a scatterplot of BI against percentile (black dots) and a fitted SCAM curve (red line).

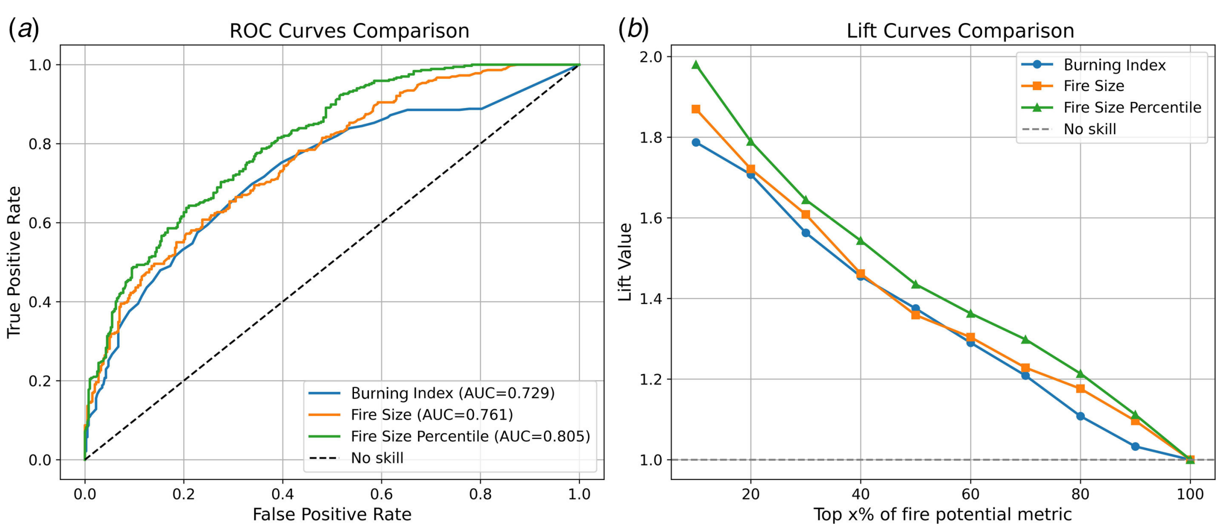

Fig. 7. Comparison of the predictive performance of three fire danger metrics (Burning Index, simulated daily fire size and fire size percentile) in predicting large wildfire occurrences. (*a*) Receiver Operating Characteristic (ROC) curves and the Area Under the Curve (AUC) values indicating overall prediction performance. (*b*) Lift curves showing the ratio of the wildfire occurrence rate within the top 10, 20, …, 100% of each fire potential metric to the overall fire occurrence rate.

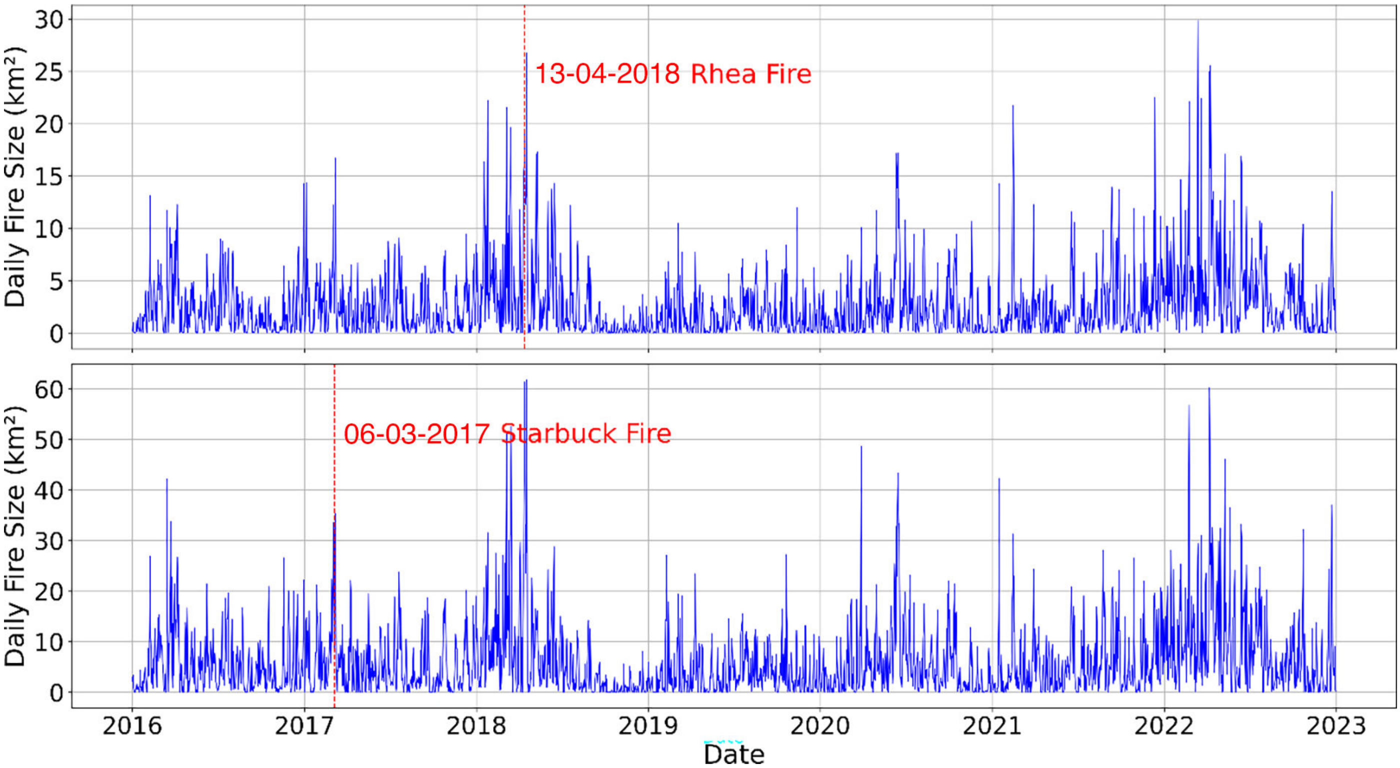

Fig. 8. Daily variations of the simulated fire size from 2016–2022 in the Rhea Fire hexagon (Fig. 3*b*) and the Starbuck Fire hexagon (Fig. 3*c*). Red dashed lines indicate the critical growth dates of the Rhea Fire (13 April 2018) and the Starbuck Fire (6 March 2017).

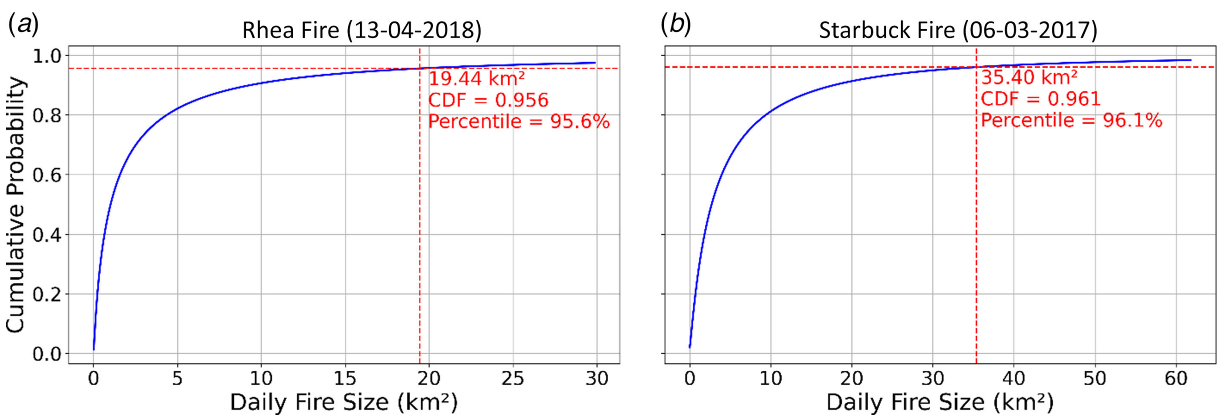

Fig. 9. Cumulative probability curves of the fitted log-normal distributions for simulated daily fire sizes (2016–2022) within the Rhea Fire hexagon (Fig. 3*b*) and the Starbuck Fire hexagon (Fig. 3*c*). Red dashed lines indicate the simulated fire size, cumulative probability and percentile on the respective critical growth dates of the Rhea Fire (13 April 2018) and the Starbuck Fire (6 March 2017). These two fires were selected for retrospective fire danger assessment using the new system.

and spread eastward to Oklahoma, showed particularly elevated fire activities on 26 February 2024. As shown in Fig. 11*a*, the large fire size and high fire danger level were concentrated in the Texas Panhandle. Specifically, the simulated fire size in the Smokehouse Creek Fire hexagon (Roberts County, TX) reached 17.7 km^2, placing it at the 89.2nd percentile of all daily fire size values (Fig. 12*a*). Likewise, Fig. 11*b* shows the elevated fire size across western and central Oklahoma and Texas on 14 March 2025. On this date, the simulated fire size in the Cottonwood Fire hexagon (Payne County, Oklahoma) reached 13.7 km^2, corresponding to the 77.4th percentile (Fig. 12*b*). These results demonstrate that the WDAF, when driven by NAM weather forecasts, effectively captured elevated fire danger

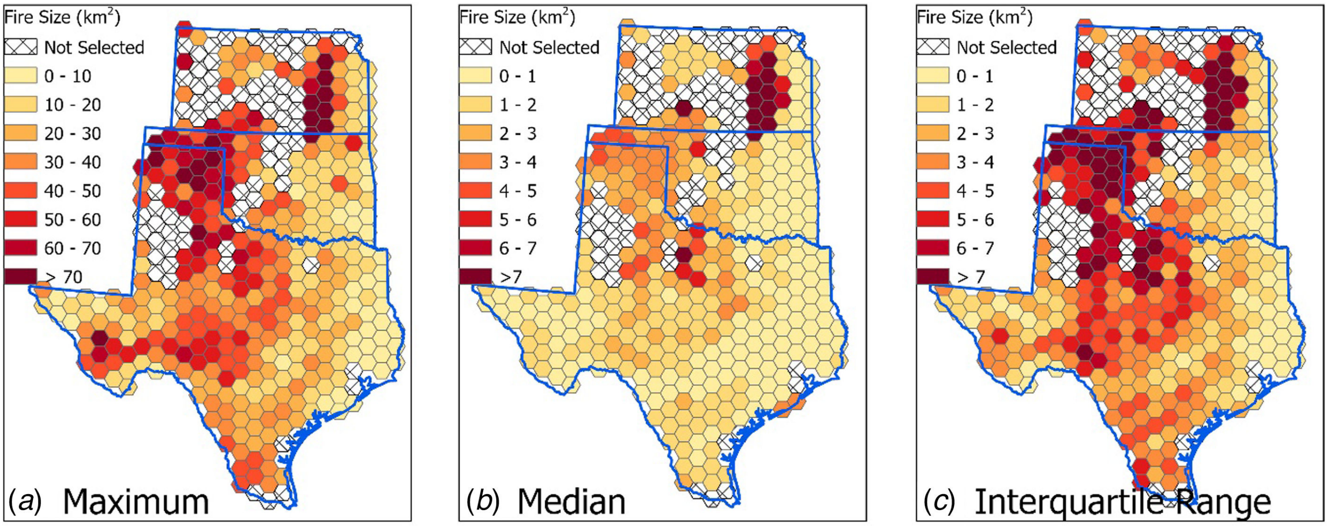

Fig. 10. Climatology of fire danger, represented by the maximum (*a*), median (*b*), and interquartile range (*c*) of simulated daily fire sizes from 2016–2022. Note: the sequential color scale and numerical bin ranges are to highlight spatial gradients and emphasize the hexagons with large fire sizes (dark red), rather than to represent operational decision-making thresholds.

conditions on the critical growth dates of two large wildfire events. This alignment between simulated fire size and actual fire events underscores the WDAF's potential as an operational tool for forecasting high-risk fire days.

Discussion

Contributions and advantages of the WDAF framework

By developing and validating a novel fire simulation-based framework, this study lays the groundwork for a robust and adaptable approach to wildfire danger assessment and forecasting. The WDAF framework offers several advantages:

- It enhances daily fire danger quantification by directly linking it to simulated fire sizes and their corresponding percentiles, which makes the information more intuitive for end users to understand.
- The estimated fire size percentile allows for normalizing daily fire size according to fire spread simulations over a historical baseline period, providing a relative measure of fire danger anomaly adaptable to regional differences in fire regimes.
- The simulation-based approach captures the influences of spatial variability in fuels and topography, as well as time-varying weather conditions, on fire behavior and propagation. This enables a realistic and accurate estimation of fire spread potentials, particularly in landscapes with complex terrain and diverse fuelbeds.

Framework configuration and regional adaptation

The WDAF framework is designed for flexibility, allowing users to choose the most appropriate fire model, input datasets, and statistical methods for fitting the distribution of daily fire sizes and calculating percentiles. Users can also define the spatial resolution of simulation grids and the number of ignition points to simulate fire behavior and spread dynamics. Besides a regular grid, the framework can be configured within administrative units (e.g. fire alert zones, counties, or municipalities) to report fire danger levels at these jurisdictional scales and support jurisdiction-based decision-making.

The core components required to implement WDAF include: (1) a spatially explicit fire model, (2) landscape maps of topography and fuel types, (3) continuous historical hourly weather data for the baseline period, and (4) target-day weather forecasts. Several parameters remain flexible and need to be adjusted based on regional characteristics and computational constraints, including the choice of fire model, spatial resolution, number and distribution of ignition points, and the statistical distribution function to calculate fire size percentiles. Table 2 lists a range of fire models, weather and fuel products, and statistical distribution approaches that could be potentially integrated within the WDAF.

When applying the WDAF framework to new regions, several practical considerations should be evaluated, including computational constraints, data availability and statistical modeling.

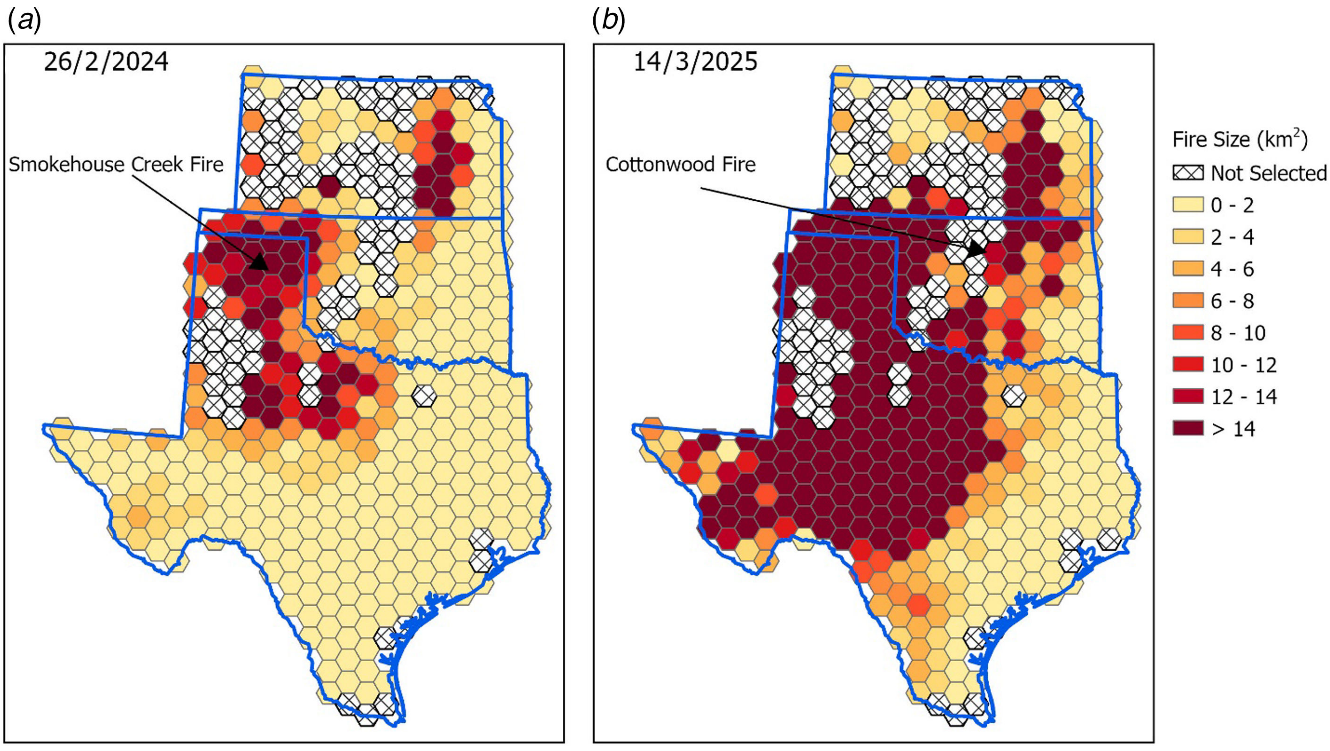

Fig. 11. The forecasted daily fire size (km^2) by the Wildfire Danger Assessment and Forecast (WDAF) framework driven by the North America Mesoscale (NAM) weather data for two days of 26 February 2024 (*a*) and 14 March 2025 (*b*). Note: the sequential color scale and numerical bin ranges are to highlight spatial gradients and emphasize the hexagons with large simulated fire sizes (dark red), rather than to represent operational decision-making thresholds.

Table 2. Potential fire behavior models, input datasets, and statistical distribution models that could be used in the wildfire danger assessment and forecast (WDAF) framework.

Fire behavior model	FARSITE, wildfire analyst, WRF-fire, FIRETEC, prometheus
Input data: historical weather	NARR, NCEP/NCAR, MERRA, ERA5, RTMA
Input data: forecast weather	NAM, HRRR, NDFD
Input data: fuel type and loading	LANDFIRE (U.S.) and FCCS (global)
Statistical distributions	Power law, log-normal, exponential

- Computational constraints: in addition to FARSITE, several other fire modeling systems could be integrated into the WDAF framework, including Wildfire Analyst (Monedero *et al.* 2019), WRF-Fire (Coen *et al.* 2013), FIRETEC (Koo *et al.* 2012) and Prometheus (Tymstra *et al.* 2010). However, it is important to note that, while integrating fully physical-based fire models (e.g. FIRETEC, WRF-Fire) is theoretically possible, their application at regional scales such as the SGP remains operationally challenging. The significant computational demands associated with simulating thousands of fire events on a daily basis necessitate the use of more efficient fire behavior models (e.g. FARSITE) for large-scale applications. Selecting a highly complex computational fluid dynamics model or increasing the density of hypothetical ignitions will improve realism but may render daily operational forecasting computationally prohibitive over large spatial domains. Accordingly, users are expected to carefully choose fire models and adjust ignition density based on their domain and available computational resources.
- Weather and Fuel Data Availability: for the retrospective fire danger assessment, potential sources of hourly weather input include the NARR (Mesinger *et al.* 2006), the NCEP/NCAR Reanalysis (Kalnay *et al.* 2011), the Modern-Era Retrospective analysis for Research and Applications (MERRA) (Gelaro *et al.* 2017), ERA5 from the European Centre for Medium-Range Weather Forecasts (Hersbach *et al.* 2020), Real-Time Mesoscale Analysis (RTMA) (De Pondeca *et al.* 2011), etc. As the NAM weather forecast approaches retirement, it is necessary to transition to alternative weather input datasets, such as the High-Resolution Rapid Refresh (HRRR) (Dowell *et al.* 2022) and the National Digital Forecast Database (NDFD) (Glahn and Ruth 2003), which provide short-term, high-resolution weather forecasts necessary for operational applications. For fuel input, the LANDFIRE project provides 30 m resolution fuel maps across the US (Rollins 2009). At the global scale, fuel bed maps developed based on the Fuel Characteristic Classification System

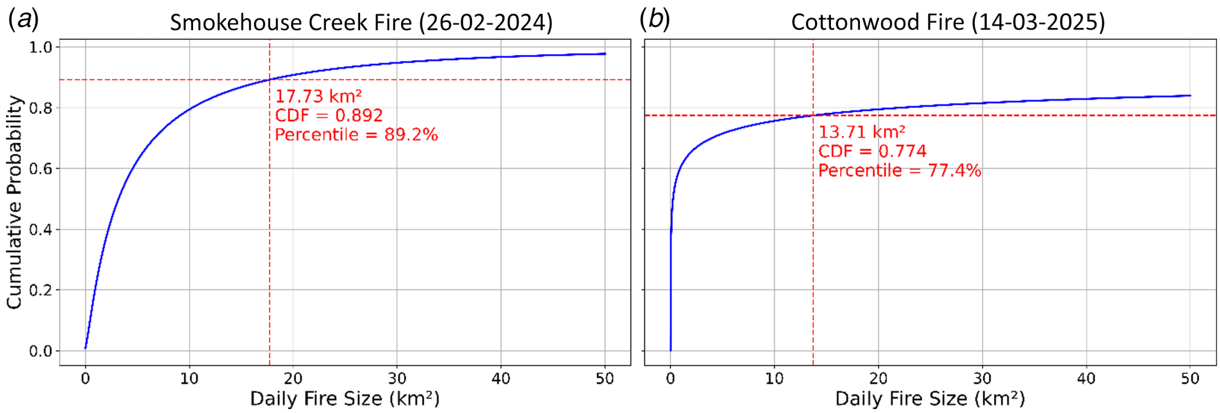

Fig. 12. Cumulative probability curves of the fitted log-normal distributions for simulated daily fire sizes (2016–2022) within the Smokehouse Creek Fire hexagon (Fig. 3*a*) and the Cottonwood Fire hexagon (Fig. 3*d*). Red dashed lines indicate the forecasted fire size, cumulative probability and percentile on the respective critical growth dates of the Smokehouse Creek Fire (26 February 2024) and the Cottonwood Fire (14 March 2025). These two fires were selected to evaluate the capacity of the new system to forecast fire danger.

(FCCS) (Pettinari and Chuvieco 2016) could be used to support the application of the WDAF framework in other countries. While the US benefits from high-resolution, frequently updated fuel products like LANDFIRE, applying this framework in other regions may require reliance on coarser datasets like FCCS or the development of new dataset.

- Statistical Modeling: fire size distributions are typically highly skewed (Hantson *et al.* 2015). Common statistical approaches to model these distributions include the power law, log-normal and exponential distributions (Cumming 2001; Hantson *et al.* 2015; Yang *et al.* 2015). Users need to evaluate these methods and select the one that best fits the fire size characteristics for their specific region.

Operational considerations and challenges

Timely update of input data

Fuel conditions and weather data are both time-varying, with weather exhibiting rapid fluctuations and requiring frequent updates. Effective operational fire danger forecasting depends on access to up-to-date weather forecasts. To ensure the framework operates in a timely and consistent manner, it is necessary to develop automated procedures for acquiring and preprocessing weather data. In contrast to weather, fuel types typically change over longer timescales (months to years), influenced by factors such as land use, natural disturbances and long-term climate change (Fares *et al.* 2017). Because the WDAF framework is explicitly designed for retrospective analysis and short-term fire potential forecasting rather than future projections over a long period, it relies heavily on the accuracy of current landscape conditions. Therefore, when using LANDFIRE fuel data within the WDAF framework, it is important to incorporate the more recent version, which is updated annually, to capture recent disturbances and ensure the reliability of fire danger forecasts. Additionally, changing climate conditions are expected to alter regional fire regimes, which makes it necessary to extend the baseline period to update the characteristics of fire sizes.

Computational demand

Simulating spatially explicit fire behavior and fire spread across large landscapes at fine temporal and spatial resolutions poses substantial computational challenges. In the demonstration, the SGP application required over 7 million individual FARSITE simulations (2557 days × 356 hexagons × 8 ignition points per hexagon) to establish the 7 year daily historical baseline (Step 2 of the WDAF framework, Fig. 1), highlighting the substantial computational burden. This challenge is more pronounced for operational fire potential forecasting. In an operational setting, fire managers require rapid turnaround to support timely management decision-making. Thousands of simulations must be executed, aggregated and visualized in a narrow time window following the release of daily weather forecasts. To improve efficiency, we developed a Python-based program that enables FARSITE to run in parallel mode. However, using eight ignition points per hexagon may be insufficient to adequately capture average fire spread conditions in highly heterogeneous landscapes. As operational computing capacity increases, users could set more ignition points to provide more robust stochastic sampling. Overcoming these computational constraints will be critical for operational applications of WDAF framework at a large scale.

Result interpretation and 'False Positives'

A known challenge in fire danger rating system is the occurrence of 'False Positives', where high fire danger is predicted but no fires occur (Ardid *et al.* 2026). WDAF outputs should be interpreted as an indicator of fire spread potential, rather than a prediction of fire occurrence. This is because the developed WDAF framework is based on fire spread simulations of hypothetical, randomly distributed ignitions in each grid and estimates fire size if an ignition were to occur. In reality, the occurrence of large wildfires is an extremely rare event, which needs the cooperation of fire weather and fuel conditions and the availability of ignition sources. It is possible that, even when environmental conditions are highly favorable for fire spread, no fire event will occur due to the absence of ignition sources (e.g. human activity, lightning, or wind-driven powerline failures). Therefore, a day with high fire potential but no observed fire occurrence does not necessarily reflect a deficiency in the framework. The ability of WDAF to predict actual fire occurrence could be improved by coupling WDAF outputs with ignition probability models (e.g. Bar Massada *et al.* 2011; Catry *et al.* 2009; Dorph *et al.* 2022; Muhs *et al.* 2020), which enables integrated assessments of both fire occurrence probability and spread potential.

Limitations and future development

The WDAF fire potential metrics showed good performance in capturing large wildfire occurrences across the SGP, supporting the validity of the WDAF framework as a tool for fire danger assessment. However, several limitations remain and motivate future model development. First, additional evaluation is needed to assess the performance of WDAF metrics across diverse regions and fire regimes. Future validation efforts should incorporate comparison between simulated daily fire sizes and independent datasets, including historical fire records or satellite observations (e.g. Picotte *et al.* 2016; Giglio *et al.* 2018; Short 2022).

In this study, the WDAF framework quantifies fire spread potential using daily fire size simulations. It is noteworthy that fire behavior models also generate other outputs, such as fireline intensity and flame length, which may provide complementary information to enhance characterization of fire potential. By integrating forecasted fire spread and intensity metrics with geospatial datasets representing population density, infrastructure and critical wildlife habitats, future iterations of the WDAF could enable explicit assessment of wildfire exposure and vulnerability, thereby supporting operational fire risk forecasting and quantification of potential socioeconomic and ecological impacts (Scott *et al.* 2013).

Uncertainty in meteorological input represents another important limitation. Grid products such as NARR and NAM have relatively coarse spatial resolution, which can smooth localized extreme wind events. Previous studies showed that NARR systematically underestimates wind speeds (Hoover *et al.* 2014), potentially leading to underestimation of fire sizes. Although the WDAF framework partially mitigates this bias by relying on the simulated fire size percentiles, wind-related uncertainties remain, particularly in regions such as the SGP where extreme wind events are common and cause powerline failures and destructive megafires. Incorporating higher-resolution wind datasets or near-real-time meteorological measurements could improve representation of extreme fire behavior and enhance prediction of rapid fire spread and megafire occurrence.

Fuel moisture representation introduced limitations. In this study, live fuel moisture for herbaceous and woody fuels was kept static (at 80 and 9, respectively) based on FARSITE default settings, which did not capture seasonal variability. In grass-dominated ecosystems, seasonal variations in live fuel moisture profoundly affect fire behavior and spread rate. As a result, the simulated variability in fire danger metrics was primarily driven by weather, fuel type and dead fuel moisture. Future applications should incorporate dynamic live fuel moisture estimates, which could be derived from satellite observations (e.g. Yebra *et al.* 2013; Rao *et al.* 2020) or from the output of empirical models (e.g. Jolly *et al.* 2024). Additionally, the initialization of dead fuel moisture and the relatively short 24 h model spin-up period may be insufficient for coarse fuels (e.g. 1000 h fuels) to equilibrate with environmental conditions, limiting the framework's ability to capture the effects of prolonged drought on fire behavior. Future implementations could incorporate continuous fuel moisture modeling approaches (e.g. Nelson 2000) to more accurately initialize heavy fuel moisture and to improve model robustness.

The use of static fuel maps represents another constraint. In this study, heavily agricultural regions were excluded from the evaluation, despite their potential risk during the non-growing season. Integrating seasonally dynamic fuel maps that allow agricultural areas to transition between burnable and non-burnable states would enable the framework to better represent and forecast fire danger in agriculture-dominated landscapes.

Finally, several uncertainties are related to the placement of ignitions and the summarization of simulation outputs. The framework relies on randomly distributed ignitions to assess generalized fire spread potential across the landscape, which may undersample the most hazardous fuel configurations. Future implementations could refine ignition placement by considering the pattern of wildfire susceptibility. In addition, the current framework summarizes multi-ignition simulations using the mean value to represent generalized fire size. Because fire suppression resources are often allocated based on worst-case scenarios, capturing the potential of high-impact, large fires within a landscape may provide more actionable information for fire management. Therefore, future versions could consider alternative statistical metrics for summarization, such as the maximum or the 90th percentile of simulated fire sizes in a grid.

Conclusions

Wildfires cause severe economic losses and ecological impacts across many regions worldwide, underscoring the need for more reliable fire danger assessment and forecasting tools. In this study, we developed a new framework for fire danger assessment and forecasting based on simulations of fire spread and daily fire size using a fire behavior model. Application of this framework in the SGP demonstrated that the derived fire metrics effectively captured the occurrence of major fires, highlighting its potential as a complementary tool to the widely used empirical fire danger rating systems for fire potential evaluation and forecast.

Supplementary material

Supplementary material can be access from the article page online.

References

Abatzoglou JT (2013) Development of gridded surface meteorological data for ecological applications and modelling. *International Journal of Climatology* 33(1), 121–131. doi:10.1002/joc.3413

Ager AA, Vaillant NM, Finney MA (2011) Integrating fire behavior models and geospatial analysis for wildland fire risk assessment and fuel management planning. *Journal of Combustion* 2011(1), 572452. doi:10.1155/2011/572452

Andela N, Morton DC, Giglio L, Paugam R, Chen Y, Hantson S, van der Werf GR, Randerson JT (2019) The global fire atlas of individual fire size, duration, speed and direction. *Earth System Science Data* 11(2), 529–552. doi:10.5194/essd-11-529-2019

Ardid A, Power A, Valencia A, Pearce HG, Gross S, Dempsey D, Boer M (2026) From forecast skill to economic value: sub-hourly wildfire potential forecasting across Australian regions. *International Journal of Wildland Fire* 35(4). doi:10.1071/WF25221

Baker KR, Koplitz SN, Foley KM, Avey L, Hawkins A (2019) Characterizing grassland fire activity in the Flint Hills region and air quality using satellite and routine surface monitor data. *Science of The Total Environment* 659, 1555–1566. doi:10.1016/j.scitotenv.2018.12.427

Balch JK, Iglesias V, Mahood AL, Cook MC, Amaral C, DeCastro A, Leyk S, McIntosh TL, Nagy RC, St Denis L, Tuff T, Verleye E, Williams AP, Kolden CA (2024) The fastest-growing and most destructive fires in the US (2001 to 2020). *Science (New York, NY)* 386(6720), 425–431. doi:10.1126/science.adk5737

Bar Massada A, Radeloff VC, Stewart SI, Hawbaker TJ (2009) Wildfire risk in the wildland–urban interface: a simulation study in northwestern Wisconsin. *Forest Ecology and Management* 258(9), 1990–1999. doi:10.1016/j.foreco.2009.07.051

Bar Massada A, Syphard AD, Hawbaker TJ, Stewart SI, Radeloff VC (2011) Effects of ignition location models on the burn patterns of simulated wildfires. *Environmental Modelling & Software* 26(5), 583–592. doi:10.1016/j.envsoft.2010.11.016

Bradley AP (1997) The use of the area under the ROC curve in the evaluation of machine learning algorithms. *Pattern Recognition* 30(7), 1145–1159. doi:10.1016/S0031-3203(96)00142-2

Carlson JD, Burgan RE, Engle DM, Greenfield JR (2002) The Oklahoma fire danger model: an operational tool for mesoscale fire danger rating in Oklahoma. *International Journal of Wildland Fire* 11(4), 183–191. doi:10.1071/WF02003

Catry FX, Rego FC, Bação FL, Moreira F (2009) Modeling and mapping wildfire ignition risk in Portugal. *International Journal of Wildland Fire* 18(8), 921–931. doi:10.1071/WF07123

Chen Y, Hall J, van Wees D, Andela N, Hantson S, Giglio L, van der Werf GR, Morton DC, Randerson JT (2023) Multi-decadal trends and variability in burned area from the fifth version of the Global Fire Emissions Database (GFED5). *Earth System Science Data* 15(11), 5227–5259. doi:10.5194/essd-15-5227-2023

Chen B, Wu S, Jin Y, Song Y, Wu C, Venevsky S, Xu B, Webster C, Gong P (2024) Wildfire risk for global wildland–urban interface areas. *Nature Sustainability* 7, 474–484. doi:10.1038/s41893-024-01291-0

Choudhary R., Gianey H.K. (2017) Comprehensive review on supervised machine learning algorithms. 2017 International Conference on Machine Learning and Data Science (MLDS), IEEE, Noida, pp. 37–43

Coen JL, Cameron M, Michalakes J, Patton EG, Riggan PJ, Yedinak KM (2013) WRF-fire: coupled weather–wildland fire modeling with the weather research and forecasting model. *Journal of Applied Meteorology and Climatology*, 16–38. doi:10.1175/JAMC-D-12-023.1

Cohen JD, Deeming JE (1985) 'The national fire-danger rating system: basic equations.' (US Department of Agriculture, Forest Service, Pacific Southwest Forest and Range Experiment Station)

Coop JD, Parks SA, McClernan SR, Holsinger LM (2016) Influences of prior wildfires on vegetation response to subsequent fire in a reburned Southwestern landscape. *Ecological Applications* 26(2), 346–354. doi:10.1890/15-0775

Cumming SG (2001) A parametric model of the fire-size distribution. *Canadian Journal of Forest Research* 31(8), 1297–1303. doi:10.1139/x01-032

Cunningham CX, Williamson GJ, Bowman D (2024) Increasing frequency and intensity of the most extreme wildfires on Earth. *Nature Ecology & Evolution* 8(8), 1420–1425. doi:10.1038/s41559-024-02452-2

Deeming JE, Burgan RE, Cohen JD (1977) The national fire-danger rating system, 1978. Department of Agriculture, Forest Service, Intermountain Forest and Range Experiment Station

De Pondeca MSFV, Manikin GS, DiMego G, Benjamin SG, Parrish DF, Purser RJ, Wu W-S, Horel JD, Myrick DT, Lin Y, Aune RM, Keyser D, Colman B, Mann G, Vavra J (2011) The real-time mesoscale analysis at NOAA's National Centers for Environmental Prediction: current status and development. *Weather and Forecasting* 26(5), 593–612. doi:10.1175/WAF-D-10-05037.1

Donovan VM, Crandall R, Fill J, Wonkka CL (2023) Increasing Large Wildfire in the Eastern United States. *Geophysical Research Letters* 50(24), e2023GL107051. doi:10.1029/2023GL107051

Dorph A, Marshall E, Parkins KA, Penman TD (2022) Modelling ignition probability for human- and lightning-caused wildfires in Victoria, Australia. Other Hazards (e.g., Glacial and Snow Hazards, Karst, Wildfires Hazards, and Medical Geo-Hazards). 1–21. doi:10.5194/nhess-2022-52

Dowell DC, Alexander CR, James EP, Weygandt SS, Benjamin SG, Manikin GS, Blake BT, Brown JM, Olson JB, Hu M (2022) The high-resolution rapid refresh (HRRR): an hourly updating convection-allowing forecast model. *Part I: Motivation and System Description. Weather and Forecasting* 37, 1371–1395

Eidenshink J, Schwind B, Brewer K, Zhu Z-L, Quayle B, Howard S (2007) A project for monitoring trends in burn severity. *Fire Ecology* 3(1), 3–21. doi:10.4996/fireecology.0301003

Fang S, Yang J, Jiao X, Zou CB, Desjardins A, Yang H, Zhang Q, Hernandez A (2026) Satellite-based analysis of hourly progression and driving factors of large U.S. wildfires. *International Journal of Applied Earth Observation and Geoinformation* 149, 105288. doi:10.1016/j.jag.2026.105288

Fares S, Bajocco S, Salvati L, Camarretta N, Dupuy J-L, Xanthopoulos G, Guijarro M, Madrigal J, Hernando C, Corona P (2017) Characterizing potential wildland fire fuel in live vegetation in the Mediterranean region. *Annals of Forest Science* 74(1), 1. doi:10.1007/s13595-016-0599-5

Finney MA (1998) 'FARSITE: Fire Area Simulator-model development and evaluation (no.RMRS-RP-4). U.S.' (Department of Agriculture, Forest Service, Rocky Mountain Research Station: Ogden, UT)

Gelaro R, McCarty W, Suárez MJ, Todling R, Molod A, Takacs L, Randles C, Darmenov A, Bosilovich MG, Reichle R, Wargan K, Coy L, Cullather R, Draper C, Akella S, Buchard V, Conaty A, da Silva A, Gu W, Kim G-K, Koster R, Lucchesi R, Merkova D, Nielsen JE, Partyka G, Pawson S, Putman W, Rienecker M, Schubert SD, Sienkiewicz M, Zhao B (2017) The modern-era retrospective analysis for research and applications, Version 2 (MERRA-2). *Journal of Climate* 30(13), 5419–5454. doi:10.1175/JCLI-D-16-0758.1

Giglio L, Boschetti L, Roy DP, Humber ML, Justice CO (2018) The Collection 6 MODIS burned area mapping algorithm and product. *Remote Sensing of Environment* 217, 72–85. doi:10.1016/j.rse.2018.08.005

Glahn HR, Ruth DP (2003) The new digital forecast database of the national weather service. *Bulletin of the American Meteorological Society* 84(2), 195–202. doi:10.1175/BAMS-84-2-195

Hantson S, Pueyo S, Chuvieco E (2015) Global fire size distribution is driven by human impact and climate. *Global Ecology and Biogeography* 24(1), 77–86. doi:10.1111/geb.12246

Hantson S, Pueyo S, Chuvieco E (2016) Global fire size distribution: from power law to log-normal. *International Journal of Wildland Fire* 25(4), 403–412. doi:10.1071/WF15108

Hersbach H, Bell B, Berrisford P, Hirahara S, Horányi A, Muñoz-Sabater J, Nicolas J, Peubey C, Radu R, Schepers D, Simmons A, Soci C, Abdalla, S, Abellan X, Balsamo G, Bechtold P, Biavati G, Bidlot J, Bonavita M, De Chiara G, Dahlgren P, Dee D, Diamantakis M, Dragani R, Flemming J, Forbes R, Fuentes M, Geer A, Haimberger L, Healy S, Hogan RJ, Hólm E, Janisková M, Keeley S, Laloyaux P, Lopez P, Lupu C, Radnoti G, de Rosnay P, Rozum I, Vamborg F, Villaume S, Thépaut J-N (2020) The ERA5 global reanalysis. *Quarterly Journal of the Royal Meteorological Society* 146, 1999–2049. doi:10.1002/qj.3803

Hollis JJ, Matthews S, Anderson WR, Cruz MG, Fox-Hughes P, Grootemaat S, Kenny BJ, Sauvage S (2024) A framework for defining fire danger to support fire management operations in Australia. *International Journal of Wildland Fire* 33, WF23141. doi:10.1071/WF23141

Hoover JD, Doesken N, Elder K, Laituri M, Liston GE (2014) Temporal trend analyses of alpine data using North American regional reanalysis and in situ data: temperature, wind speed, precipitation, and derived blowing snow. *Journal of Applied Meteorology and Climatology* 53(3), 676–693. doi:10.1175/JAMC-D-13-092.1

Ivey MA, Wonkka CL, Weidig NC, Donovan VM (2024) Woody Cover Fuels Large Wildfire Risk in the Eastern US. *Geophysical Research Letters* 51(24), e2024GL110586. doi:10.1029/2024GL110586

Jolly WM, Freeborn PH, Bradshaw LS, Wallace J, Brittain S (2024) Modernizing the US National Fire Danger Rating System (version 4): simplified fuel models and improved live and dead fuel moisture calculations. *Environmental Modelling & Software* 181, 106181. doi:10.1016/j.envsoft.2024.106181

Juang CS, Williams AP, Abatzoglou JT, Balch JK, Hurteau MD, Moritz MA (2022) Rapid growth of large forest fires drives the exponential response of annual forest-fire area to aridity in the Western United States. *Geophysical Research Letters* 49(5), e2021GL097131. doi:10.1029/2021GL097131

Júnior JSS, Paulo JR, Mendes J, Alves D, Ribeiro LM, Viegas C (2022) Automatic forest fire danger rating calibration: exploring clustering techniques for regionally customizable fire danger classification. *Expert Systems with Applications* 193, 116380. doi:10.1016/j.eswa.2021.116380

Kalnay E, Kanamitsu M, Kistler R, Collins W, Deaven D, Gandin L, Iredell M, Saha S, White G, Woollen J (2011) The NCEP/NCAR 40-year reanalysis project. Renewable energy. (Routledge)

Koo E, Linn RR, Pagni PJ, Edminster CB (2012) Modelling firebrand transport in wildfires using HIGRAD/FIRETEC. *International Journal of Wildland Fire* 21(4), 396–417. doi:10.1071/WF09146

Krawchuk MA, Moritz MA, Parisien M-A, Van Dorn J, Hayhoe K (2009) Global pyrogeography: the current and future distribution of wildfire. *PLOS One* 4(4), e5102. doi:10.1371/journal.pone.0005102

Lindley TT, Speheger DA, Day MA, Murdoch GP, Smith BR, Nauslar NJ, Daily DC (2019) Megafires on the southern Great Plains. *Journal of Operational Meteorology* 7(12), 164–179. doi:10.15191/nwajom.2019.0712

MacCarthy J, Tyukavina A, Weisse MJ, Harris N, Glen E (2024) Extreme wildfires in Canada and their contribution to global loss in tree cover and carbon emissions in 2023. *Global Change Biology* 30(6), e17392. doi:10.1111/gcb.17392

McArthur AG (1967) Fire behaviour in eucalypt forests

Mesinger F, DiMego G, Kalnay E, Mitchell K, Shafran PC, Ebisuzaki W, Jović D, Woollen J, Rogers E, Berbery EH, Ek MB, Fan Y, Grumbine R, Higgins W, Li H, Lin Y, Manikin G, Parrish D, Shi W (2006) North American regional reanalysis. *Bulletin of the American Meteorological Society* 87(3), 343–360. doi:10.1175/BAMS-87-3-343

Monedero S, Ramirez J, Cardil A (2019) Predicting fire spread and behaviour on the fireline. Wildfire analyst pocket: A mobile app for wildland fire prediction. *Ecological Modelling* 392, 103–107. doi:10.1016/j.ecolmodel.2018.11.016

Muhs JW, Parvania M, Nguyen HT, Palmer JA Characterizing probability of wildfire ignition caused by power distribution lines. *IEEE Transactions on Power Delivery* 36(6), 3681–3688. doi:10.1109/TPWRD.2020.3047101

Nelson Jr, R. M. (2000) Prediction of diurnal change in 10-h fuel stick moisture content. *Canadian Journal of Forest Research* 30(7), 1071–1087. doi:10.1139/x00-032

Oliveira U, Soares-Filho B, Rodrigues H, Figueira D, Gomes L, Leles W, Miranda H (2023) A near real-time web-system for predicting fire spread across the Cerrado biome. *Scientific Reports* 13(1), 4829

Parisien MA, Kafka VG, Hirsch KG, Todd JB, Lavoie SG, Maczek PD (2005) Mapping wildfire susceptibility with the BURN-P3 simulation model. Natural Resources Canada, Canadian Forest Service. (Northern Forestry Centre, Edmonton, Alberta)

Pausas JG, Keeley JE (2021) Wildfires and global change. *Frontiers in Ecology and the Environment* 19(7), 387–395. doi:10.1002/fee.2359

Pettinari ML, Chuvieco E (2016) Generation of a global fuel data set using the Fuel Characteristic Classification System. *Biogeosciences* 13(7), 2061–2076. doi:10.5194/bg-13-2061-2016

Pettinari ML, Chuvieco E (2020) Fire danger observed from space. *Surveys in Geophysics* 41, 1437–1459. doi:10.1007/s10712-020-09610-8

Picotte JJ, Peterson B, Meier G, Howard SM (2016) 1984–2010 trends in fire burn severity and area for the conterminous US. *International Journal of Wildland Fire* 25(4), 413–420. doi:10.1071/WF15039

Pya N, Wood SN (2015) Shape constrained additive models. *Statistics and Computing* 25(3), 543–559. doi:10.1007/s11222-013-9448-7

Rao K, Williams AP, Flefil JF, Konings AG (2020) SAR-enhanced mapping of live fuel moisture content. *Remote Sensing of Environment* 245, 111797. doi:10.1016/j.rse.2020.111797

Rodrigues M, Resco de Dios V, Sil Â, Cunill Camprubí À, Fernandes PM (2024) VPD-based models of dead fine fuel moisture provide best estimates in a global dataset. *Agricultural and Forest Meteorology* 346, 109868. doi:10.1016/j.agrformet.2023.109868

Rollins MG (2009) LANDFIRE: a nationally consistent vegetation, wildland fire, and fuel assessment. *International Journal of Wildland Fire* 18(3), 235–249. doi:10.1071/WF08088

Scott J, Burgan R (2005) Standard fire behavior fuel models: a comprehensive set for use with Rothermel's surface fire spread model (no.Gen. Tech. Rep. RMRS-GTR-153). U.S. Department of Agriculture, Forest Service, Rocky Mountain Research Station, Fort Collins, CO

Scott J, Thompson M, Calkin D (2013) A wildfire risk assessment framework for land and resource management. Gen. Tech. Rep. RMRS-GTR-315. U.S. Department of Agriculture, Forest Service, Rocky Mountain Research Station, p. 83

Sharples JJ, McRae RHD, Weber RO, Gill AM (2009) A simple index for assessing fire danger rating. *Environmental Modelling & Software* 24(6), 764–774. doi:10.1016/j.envsoft.2008.11.004

Short KC (2022) Spatial wildfire occurrence data for the United States, 1992-2020 [FPA_FOD_20221014]

Tedim F, Leone V, Amraoui M, Bouillon C, Coughlan MR, Delogu GM, Fernandes PM, Ferreira C, McCaffrey S, McGee TK, Parente J, Paton D, Pereira MG, Ribeiro LM, Viegas DX, Xanthopoulos G (2018) Defining extreme wildfire events: difficulties, challenges, and impacts. *Fire* 1(1), 9. doi:10.3390/fire1010009

Thonicke K, Spessa A, Prentice IC, Harrison SP, Dong L, Carmona-Moreno C (2010) The influence of vegetation, fire spread and fire behaviour on biomass burning and trace gas emissions: results from a process-based model. *Biogeosciences* 7(6), 1991–2011. doi:10.5194/bg-7-1991-2010

Tymstra C, Bryce RW, Wotton BM, Taylor SW, Armitage OB (2010) Development and structure of Prometheus: the Canadian wildland fire growth simulation model. Natural Resources Canada, Canadian Forest Service, Northern Forestry Centre, Information Report NOR-X-417 (Edmonton, AB)
Van Auken OW (2009) Causes and consequences of woody plant encroachment into western North American grasslands. *Journal of Environmental Management* 90(10), 2931–2942. doi:10.1016/j.jenvman.2009.04.023
Van Wagner CE (1987) Development and structure of the Canadian forest fire weather index system (Forestry Technical Report No. 35). Canadian Forestry Service, Ottawa, Canada
Walding NG, Williams HTP, McGarvie S, Belcher CM (2018) A comparison of the US National Fire Danger Rating System (NFDRS) with recorded fire occurrence and final fire size. *International Journal of Wildland Fire* 27(2), 99–113. doi:10.1071/WF17030
Wood SN (2017). Generalized additive models: an introduction with R (Chapman and Hall/CRC: New York). Available at https://doi.org/10.1201/9781315370279
Yang J, Tian H, Tao B, Ren W, Lu C, Pan S, Wang Y, Liu Y (2015) Century-scale patterns and trends of global pyrogenic carbon emissions and fire influences on terrestrial carbon balance. *Global Biogeochemical Cycles* 29(9), 1549–1566. doi:10.1002/2015GB005160
Yang J, Tian H, Tao B, Ren W, Pan S, Liu Y, Wang Y (2015) A growing importance of large fires in conterminous United States during 1984–2012. *Journal of Geophysical Research* 120(12), 2625–2640. doi:10.1002/2015JG002965
Yang J, Pan S, Dangal S, Zhang B, Wang S, Tian H (2017) Continental-scale quantification of post-fire vegetation greenness recovery in temperate and boreal North America. *Remote Sensing of Environment* 199, 277–290. doi:10.1016/j.rse.2017.07.022
Yebra M, Dennison PE, Chuvieco E, Riaño D, Zylstra P, Hunt ER, Danson FM, Qi Y, Jurdao S (2013) A global review of remote sensing of live fuel moisture content for fire danger assessment: moving towards operational products. *Remote Sensing of Environment* 136, 455–468. doi:10.1016/j.rse.2013.05.029
Yeo CS, Kepert JD, Hicks R (2015) 'Fire danger indices: current limitations and a pathway to better indices.' (Bushfire & Natural Hazards CRC: Melbourne, Victoria, Australia)

Data availability. Authors used the FARSITE fire behavior model (command line version) in the WDAF framework to simulate daily fire spread. The FARSITE is available in the FlamMap (https://research.fs.usda.gov/firelab/products/dataandtools/flammap) and the command line version can be obtained through contacting the model developer. Input data to drive FARSITE include fuel conditions (LANDFIRE project, https://www.landfire.gov/), weather data (NARR, https://psl.noaa.gov/data/gridded/data.narr.html) and topography (US Geological Survey (USGS) 3D Elevation Program, available from https://www.landfire.gov/). The custom Python-based program developed to run FARSITE in parallel mode, along with sample configuration scripts used in the case study, are publicly available through FigShare, https://doi.org/10.6084/m9.figshare.32002455.

Declaration of use of AI. The author declares the use of ChatGPT to assist with grammar checking and improving the readability of this manuscript.

Conflicts of interest. The authors declare that they have no conflicts of interest.

Declaration of funding. This work was supported by the Oklahoma NSF EPSCoR S3OK project (No. OIA-1946093), the US National Science Foundation Rural Confluence (No. 2316366), USGS South Central Climate Adaptation Science Center grant (G23AC0454), Joint Fire Science Program grant (23-2-01-9) and NASA (80NSSC24K1258).

Author affiliations
[A]Department of Natural Resource Ecology and Management, Oklahoma State University, Stillwater, OK, USA.
[B]Department of Plant and Soil Sciences, Oklahoma State University, Stillwater, OK, USA.
[C]Center for Forest Disturbance Science, USDA Forest Service, Athens, GA, USA.
[D]NOAA/National Weather Service, Norman, OK, USA.
[E]Oklahoma Forest Services, Oklahoma City, OK, USA.